

# ON SCALING THEORIES OF SPACE-TIME RAINFALL: SOME RECENT RESULTS AND OPEN PROBLEMS

EFI FOUFOULA-GEORGIU  
*St. Anthony Falls Laboratory*  
*Mississippi River and Third Avenue S.E.*  
*University of Minnesota*  
*Minneapolis, MN 55414, USA*

In this paper some recent advances on rainfall scaling research are reviewed for the purpose of illustrating some important recent findings but still yet the need for further mathematical and empirical analyses to integrate results of different studies towards a comprehensive and coherent picture of the rainfall process. Our review centers around two major issues: (a) temporal rainfall and scaling, and (b) spatial rainfall scaling and relations to physical parameters of the storm environment. Some important recent developments on integrated space-time scaling descriptions are not reviewed herein as such descriptions have only recently emerged and deserve a separate focused treatment in the near future.

## 2.1 Introduction

Rainfall being the result of complex atmospheric phenomena, possesses a complicated temporal and spatial structure. A wide range of frequency-content features and extreme variability over time intervals from a few seconds to years and length intervals of a few kms to several hundred of kms, make rainfall an intriguing and challenging process to study.

Significant success of scaling models in studying various physical processes (for instance, Kolmogorov's  $5/3$  law for the energy spectrum in turbulent flows, and Brownian motion to model molecular diffusion) has motivated hydrologists to look for scale invariance in hydrologic processes, in general, and rainfall in particular. By scale invariance, it is understood that a change in the scale of description leads to processes that look statistically similar apart from factors involving the ratios of scales under study. Scaling models of rain provide attractive and parsimonious representations over a large range of scales and are supported by empirical evidence and theoretical arguments that rainfall exhibits scale-invariant symmetry (e.g., Schertzer and Lovejoy 1987; Gupta and Waymire 1990; Kumar and Foufoula-Georgiou 1993b). Scaling models explored to date for the description of temporal and spatial rainfall include fractal models of rain areas, monofractal and multifractal fields (including universal multifractals), generalized scale-invariant models, and scaling-in-fluctuations models. A review of these developments from 1991 to 1994 and references to previous works can be found in Foufoula-Georgiou and Krajewski (1995).

In this paper some recent advances on rainfall scaling research will be reviewed for the purpose of illustrating some important recent findings but still yet the need for further mathematical and empirical analyses to integrate results of different studies towards a comprehensive and coherent picture of the rainfall process. It is of course recognized that space and time variations of rainfall are not independent of each other and thus simultaneous space-time scaling descriptions of rainfall should be sought. In fact, the early studies of space-time point process models of rainfall (e.g., Waymire *et al.* 1984) were motivated by the need to integrate the temporal and spatial rainfall descriptions into a unifying modeling framework which can also explain theoretically Taylor's hypothesis of turbulence (found empirically to hold for rainfall for time scales of less than approximately 40 mins; Zawadzki 1973). Although developments in space-time models of rainfall based on the stochastic point process framework have been studied for some time now (e.g., see Cox and Isham, this volume, for newest developments), theories of space-time rainfall based on scaling ideas have only recently emerged (e.g., see Over and Gupta 1996; Marsan *et al.* 1996, Venugopal *et al.*, 1997) and were not included in this review. Rather, our discussions will center around two major issues: (a) temporal rainfall and scaling, and (b) spatial rainfall scaling and relations to physical parameters of the storm environment.

## 2.2 High-Resolution Temporal Rainfall: Scaling or Not?

### 2.2.1 Preliminaries

The temporal structure of rainfall at a point has been the subject of intense study over the past two decades. Markovian-type structures for hourly and daily rainfall formed the core of early models used to describe rainfall's extreme variability (e.g., Gabriel and Neumann 1962). The structure and the parameters of these models depended heavily on the time scale chosen for representing the rainfall process. This limitation, together with the desire to develop model structures that can handle space and time variability simultaneously, led to the formulation of continuous-time conceptual point-process rainfall models, which would be applicable over several time scales (e.g., see Foufoula-Georgiou and Georgakakos 1991 for a review of point process models up to 1990 and Onof and Wheater 1993 for a more recent reference). The hope was that this continuous-time rainfall parameterization would shed light on the underlying rainfall-generating mechanism, especially if it came from a space-time formulation. However, although valid simulation models, they provided a limited understanding of the underlying structure of the rainfall

process. The reason was that the rainfall structure was mostly imposed based on a radar-inferred phenomenology, e.g. embedding of high-intensity rain cells within lower intensity mesoscale areas (clustering), rather than truly unraveled statistically from the rainfall fields. Another practical problem with these models was that there were too many parameters embedded in the model structure, resulting in non-uniqueness and non-identifiability when the models were fitted to rainfall observations at different scales. For example, fitting the same continuous-time model to hourly or daily accumulations could result in different estimates of the model parameters rendering thus any physical meaning of these parameters questionable (e.g., see Foufoula-Georgiou and Guttorp 1987). More recent versions of point process models seem to have overcome these problems with improved model structures and parameter estimation procedures. Some recent developments in point process-based rainfall models are discussed in this volume by Cox and Isham.

Temporal rainfall exhibits extreme variability over scales of several seconds to days to years, to centuries. For example, Figure 2.1a shows a plot of rainfall intensities sampled every 5 seconds from an optical raingauge in Iowa City (see Georgakakos *et al.* 1994 for information on the data collection procedures), while Figures 2.1b, c, and d show the temporal rainfall variability over hours, months and years, respectively for an Iowa City station. Obviously, rainfall has some characteristic scales which relate, for example, to storm and interstorm duration, and seasonal periodicity. The effects of these characteristic scales must be removed if a quantitative comparison of the stochastic variability over scales is to be made. For our purposes, it suffices at this point to note that the rainfall process indeed exhibits a large variability over all these scales, and it is not clear visually if some underlying hidden similarities between scales do exist or not.

Our discussion in this section will concentrate on the findings of a couple of recent studies that have analyzed high resolution (seconds to minutes sampling interval) rainfall series for the purpose of unraveling scaling characteristics. It is interesting to note that some of these studies have been based on the same Iowa City high resolution data but still have resulted in different interpretations and conclusions which have not yet reached a point of complementarity and integration towards a better understanding of the rainfall process. To illustrate this point and outline several still open problems, we will elaborate below on the methodologies and findings of the studies by Georgakakos *et al.* (1994), Olsson *et al.* (1993), Veneziano *et al.* (1996), Menabde *et al.* (1997), Kumar (1996), Venugopal and Foufoula-Georgiou (1996) and Cârsteanu and Foufoula-Georgiou (1996). First, some basics on the mathematical methods of analysis (specifically, multiscaling and multiplicative cascades, and multireso-

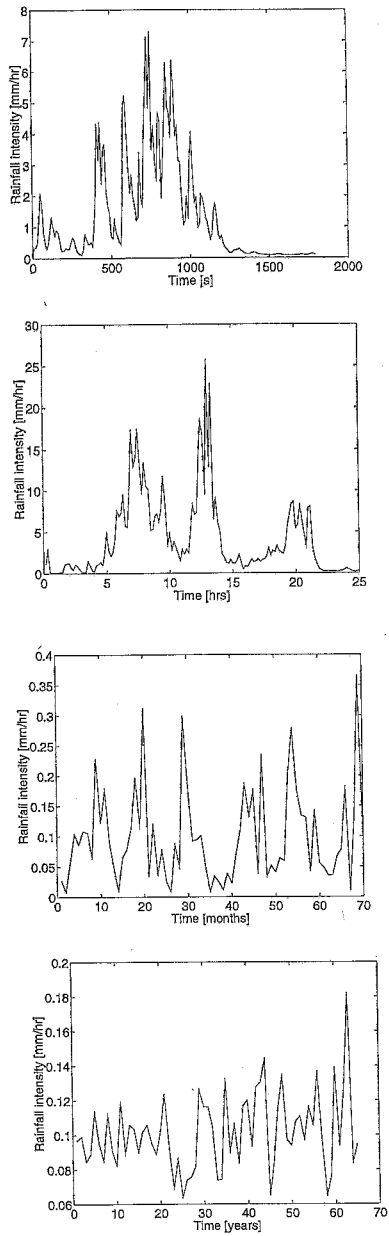


Figure 2.1: Illustration of temporal rainfall variability at scales ranging from seconds to years for an Iowa City station.

lution wavelet analysis) which are needed for our discussion are given. These are followed-up by a review and comparison of recent findings and discussion of open problems.

### 2.2.2 Mathematical background

#### Simple scaling, multiscaling and multiplicative cascades

Consider a function  $\mu$  defined on subintervals of the time axis by the values of a continuous-time, real-valued stochastic process  $X(t)$ , such that

$$\mu_t(\Delta t) \equiv X(t + \Delta t) - X(t). \quad (2.1)$$

$\mu$  is said to be self-similar ( $X(t)$  to exhibit self-similarity or simple scaling in its increments; although sometimes by an abuse of language  $X(t)$  itself is said to exhibit simple scaling) if for each  $\lambda > 0$ , there exists a constant  $C_\lambda$  such that the finite dimensional distribution of  $\mu$  satisfies the equation

$$\begin{aligned} P(C_\lambda^{-1}\mu_{t_1}(\lambda\Delta t) \leq x_1, \dots, C_\lambda^{-1}\mu_{t_n}(\lambda\Delta t) \leq x_n) = \\ P(\mu_{t_1}(\Delta t) \leq x_1, \dots, \mu_{t_n}(\Delta t) \leq x_n) \end{aligned} \quad (2.2)$$

where  $P$  is the probability measure associated with the occurrences of different values of  $\mu$ .

Notice that (2.2) has been historically defined for processes with independent increments (although it is satisfied by other processes too, such as fractional Brownian motion) which reduces the equality of the finite-dimensional distribution to an equality of their marginals. Adding to independence the requirement of identically distributed increments, results in stationarity in the increments (and in fact, also implies ergodicity) and reduces (2.2) to

$$P(C_\lambda^{-1}\mu(\lambda\Delta t) \leq x) = P(\mu(\Delta t) \leq x) \quad (2.3)$$

which is equivalently expressed as

$$\{C_\lambda^{-1}\mu(\lambda\Delta t)\} \stackrel{d}{=} \{\mu(\Delta t)\} \quad (2.4)$$

where  $\stackrel{d}{=}$  denotes equality in distribution. It can be shown that since  $C_\lambda$  satisfies  $C_{\lambda_1\lambda_2} = C_{\lambda_1}C_{\lambda_2}$ , the continuous solution of this equation follows from homogeneity as  $C_\lambda = \lambda^H$ ,  $H \in \mathbb{R}^+$  (i.e., any continuous solution of  $C_\lambda$  is a power law; see Lamperti 1962, theorem 1 for a rigorous derivation). Therefore, equation (2.3) can be equivalently written as

$$\{\mu(\lambda\Delta t)\} \stackrel{d}{=} \{\lambda^H\mu(\Delta t)\} \quad H \in \mathbb{R}^+. \quad (2.5)$$

From equation (2.5) we expect that the absolute values of moments, if they exist, will satisfy

$$E[|\mu(\lambda\Delta t)|^q] = \lambda^{qH} E[|\mu(\Delta t)|^q]. \quad (2.6)$$

Taking logarithms in (2.6) we obtain:

$$H = \frac{\log E[|\mu(\lambda\Delta t)|^q] - \log E[|\mu(\Delta t)|^q]}{q \log \lambda}. \quad (2.7)$$

Due to ergodicity, the ensemble moments can be substituted with the standard moments (i.e., moments over a realization) and since (2.7) applies for all  $\lambda$  including  $\lambda \rightarrow 0$ , it can be rewritten as

$$H = \lim_{\lambda \rightarrow 0} \frac{\log [\lambda \sum_t |\mu_t(\lambda\Delta t)|^q]}{q \log \lambda} \quad (2.8)$$

Let us now introduce the exponents  $\tau(q)$  which are defined by

$$\tau(q) \equiv - \lim_{\lambda \rightarrow 0} \frac{\log \sum_t |\mu_t(\lambda\Delta t)|^q}{\log \lambda}. \quad (2.9)$$

The spectrum of exponents  $\tau(q)$  measures how the  $q^{\text{th}}$  power of the structure function  $|X(t + \Delta t) - X(t)|$  varies with scale  $\lambda$ . Notice that if  $X(t)$  is nondecreasing, i.e.  $\mu_t(\Delta t) \geq 0, \forall \Delta t, \forall t$ , then  $\mu$  defines a measure in time, and the exponents spectrum of the structure function of the process  $X(t)$  also becomes the “mass” exponents spectrum of the measure  $\mu$  (the absolute values in the structure function being dropped in this case). From (2.8) and (2.9) we obtain that for a process which exhibits simple scaling in its increments and for which the increments are ergodic

$$H = \frac{1 - \tau(q)}{q} \quad (2.10)$$

or  $\tau(q) = 1 - qH$ . Such a spectrum of exponents which varies linearly with  $q$  is characteristic of processes exhibiting simple scaling, or more generally, of monoscaling processes.

It is noted that equation (2.10) which connects the descriptor of scaling  $H$  (which is based on ensemble moments in eq. (2.7)) to the descriptor  $\tau(q)$  which applies to each realization (eq. (2.9)), holds in the particular case when ergodicity in increments holds. This case encompasses most of the processes for which (2.2) holds and in fact it holds true for the most widely used solution of (2.2): the process of sums of independent Lévy distributed random variables, which is ergodic in its increments.

If for a process, the absolute values of moments in eq.(2.6) scale with a different exponent for each moment of order  $q$ , then  $\tau(q)$  is not a linear function

of  $q$  and the increment-process is said to exhibit multiscaling, and if  $X(t)$  is nondecreasing, then the measure  $\mu$  is called a multifractal. This amounts to a curvilinear (strictly convex) spectrum of exponents  $\tau(q)$ , and consequently to a nontrivial spectrum of scaling exponents  $f(\alpha)$ , which is connected to  $\tau(q)$  (under suitable existence conditions) by the Legendre transform

$$\alpha(q) = -\frac{d\tau(q)}{dq}$$

$$f(\alpha) = \min_q \{q\alpha(q) + \tau(q)\}. \quad (2.11)$$

The interpretation of  $f(\alpha)$  is that of a Hausdorff dimension of the set of points with Hölder exponent equal to  $\alpha$  (for which reason  $f(\alpha)$  is also called “spectrum of singularities”). Notice that in the monoscaling case, the spectrum  $f(\alpha)$  degenerates to a point, since the only valid Hölder exponent is  $\alpha = H$ . This again shows the one-to-one connection between multiscaling and multifractality, since a curved spectrum of mass exponents implies the existence of an entire range of values where  $f(\alpha)$  is defined. Also, the spectrum of dimensions  $D(q)$  (often considered for positive processes and  $q \geq 0$ ), which can be defined as

$$D(q) = \frac{\tau(q)}{1-q}, \quad (2.12)$$

becomes a strictly decreasing function with  $q$ . Notice that for monofractal measures for which  $E[\mu(\Delta t)]$  exists and is finite,  $\tau(1) = 0$  (from (2.9)) and, thus, according to (2.11),  $f(\alpha) = \alpha = H$ . Therefore,  $\tau(q)$ , which is a line of slope  $H$  going through the point  $(1,0)$ , is given by  $\tau(q) = H(1-q)$ . Thus, from (2.12),  $D(q) = D = H$  is a constant. Also,  $f(\alpha) = (\alpha = H) = D$ . This is intuitively expected, since the Hausdorff dimension of the points where the field is non-zero is equal to the fractal dimension in this case.

Multifractal fields are being simulated largely by the use of multiplicative cascades. Multiplicative cascades are measures defined on the appropriate support (e.g. a surface or a time axis), showing multiscaling (or in particular cases, simple scaling). They can be described in terms of an infinite iterative construction, beginning with a given “mass” uniformly distributed over the support. Each subsequent step divides the support and generates a number of weights (equal to the “branching number” of the generator), such that mass is redistributed to each of the divided supports by multiplication with the respective weight. To achieve conservation in the ensemble average of the mass, the expected value of the sum of weights should be equal to unity. Different cascade generators have been proposed for modeling rainfall. According to the

probability distributions of their weights, the most often used are: multinomial (where the weights take a finite number of values with certain probabilities), uniform, and lognormal (see Gupta and Waymire 1993 for a review).

The lognormal cascade was first proposed by Kolmogorov (1962) and Oboukhov (1962) in the statistical theory of turbulence, and has the property that it is the limiting measure for any generator with weights whose distribution has all moments finite. Another cascade model, used by Lovejoy and Schertzer (1987, and subsequent work), is the log-Lévy model, in which the logarithms of the weights are distributed according to a non-Gaussian stable distribution. This type of cascade produces the limiting measure for the generators with weight distributions that are attracted to Lévy-stable distributions under aggregation. A number of observations support this model versus the lognormal (see Tessier *et al.* 1993). However, as in the case of different other weight distributions that are not suitably bounded, the lack of ergodicity of models with Lévy-exponents greater than unity (Holley and Waymire 1992) also raises an estimation issue, since for real-life data it is hardly feasible to have an estimation across realizations. Apart from the probability distribution of weights in the cascade generator, the dependence structure among weights is needed to fully characterize a multiplicative cascade model. The dependence structure among weights has been explored by Gupta and Waymire (1995) and by Cârsteanu and Fofoula-Georgiou (1995, 1996), with direct application to rainfall processes.

### Time-frequency-scale analysis

A particularly useful tool for looking at a process at different scales in order to study its multiscale structure, is the wavelet transform. It has been extensively used in turbulence analysis (e.g., Fargé *et al.* 1996) and in studying other geophysical processes (e.g., see Fofoula-Georgiou and Kumar 1994 for a collection of applications). Wavelet analysis is particularly useful when a signal's frequency content changes over time and localization in both frequency and time is needed. The wavelet transform maps a one-dimensional signal into a two-dimensional plane called the time-frequency plane. The time-frequency plane is a plane defined by time which spans the signal's time domain, or part of it as necessary, and frequency which ranges from 0 to Nyquist frequency ( $= 1/2\delta$ ,  $\delta$  being the sampling interval). Time-frequency plots offer much more information about a process than the conventional temporal or power spectrum analysis only. They show what frequencies are present at what times and also what energy these frequencies carry. For example, it is interesting to note in Figure 2.2 that while two whale sounds might share almost indistinguishable



temporal and spectral density plots, their time-frequency plots provide enough information to discriminate between sounds of different whale species or happy versus sad sounds of the same whale species (Cohen 1995).

The idea of a time-frequency analysis is to “tile” the time-frequency plane (also termed phase-space) with rectangles and assign to each rectangle a magnitude representing the energy of the signal in the time-frequency interval spanned by the rectangle. The way the tiling of the plane is done depends on what kind of basis is chosen to represent the signal. Consider a rectangle centered around the point  $(t_0, \omega_0)$  as shown in Figure 2.3. The width of the rectangle in each direction represents the uncertainty with which the frequency  $\omega_0$  or time  $t_0$  can be resolved. Heisenberg’s uncertainty principle dictates that  $\sigma_\omega$  and  $\sigma_t$ , the uncertainties in frequency and time, cannot be simultaneously made arbitrarily small. Thus, if the plane were to be tiled with thin tall boxes, it means we have a very good time localization and no frequency localization. This is the case with a standard basis where the signal is represented as a superposition of *Dirac deltas*. At the other extreme, if we decide to tile the plane with wide and short boxes, this is equivalent to a Fourier representation, wherein there is optimal frequency localization and no time localization. Wavelet representations offer both good time and frequency localization (see Figure 2.4) and are therefore the basis of choice for nonstationary signals or signals whose frequency content changes over time.

Wavelets are families of functions of the form

$$\psi_{\lambda,b}(t) = \frac{1}{\sqrt{\lambda}} \psi\left(\frac{t-b}{\lambda}\right) \quad (2.13)$$

which are all generated from a single function  $\psi$  (called the mother wavelet) by translation (parameter  $b$ ) and dilation or scaling (parameter  $\lambda$ ). The factor  $1/\sqrt{\lambda}$  is a normalization factor chosen to ensure that the  $L^2$  norm of the wavelet is 1. The continuous wavelet transform of a function  $f$  is defined as (Daubechies 1992)

$$W_\psi f(\lambda, b) = |\lambda|^{-\frac{1}{2}} \int f(t) \psi\left(\frac{t-b}{\lambda}\right) dt \quad (2.14)$$

As with the Fourier transform, the wavelet transform is also invertible i.e.,

$$f(t) = \frac{C_\psi}{\lambda^2} \int_{-\infty}^{\infty} \int_{-\infty}^{\infty} W_\psi f(\lambda, b) \psi_{\lambda,b}(t) d\lambda db \quad (2.15)$$

where

$$C_\psi = 2\pi \int |\omega|^{-1} |\hat{\psi}(\omega)|^2 d\omega < \infty \quad (2.16)$$

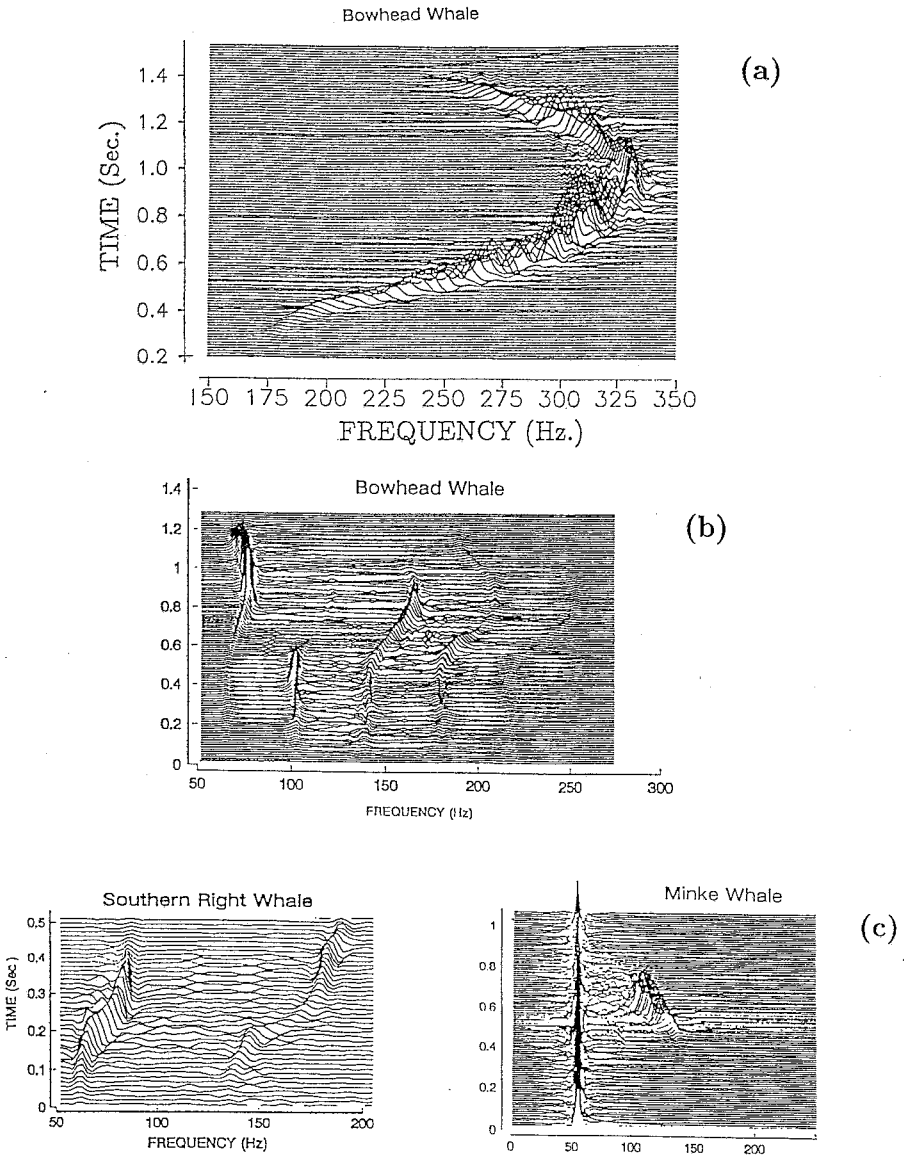


Figure 2.2: Time-frequency analysis of whale sounds: (a) time-frequency plot of a bowhead whale sound; (b) time-frequency plot of a different sound of the same whale; (c) time-frequency plots of sounds of different whales (modified from figures in Cohen 1995).

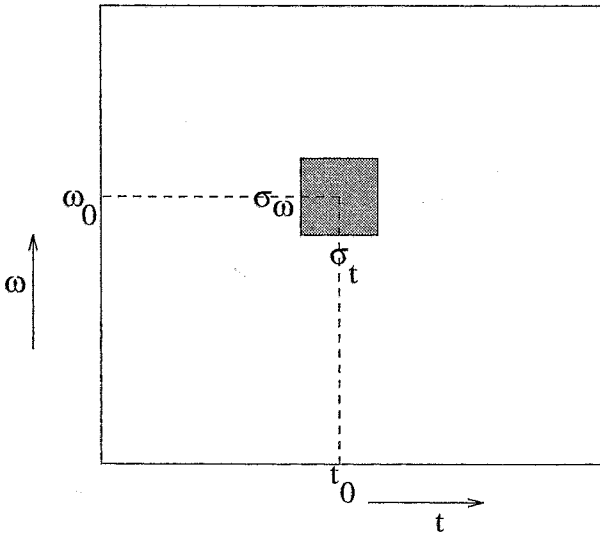


Figure 2.3: Time-frequency plane with a Heisenberg rectangle positioned at location  $(t_0, \omega_0)$ . The uncertainty of resolving time  $t_0$  is  $\sigma_t$  and the uncertainty of resolving frequency  $\omega_0$  is  $\sigma_\omega$ . According to Heisenberg's uncertainty principle  $\sigma_t$  and  $\sigma_\omega$  cannot be made simultaneously arbitrarily small i.e., increased time resolution occurs at the expense of loss in frequency resolution and vice-versa.

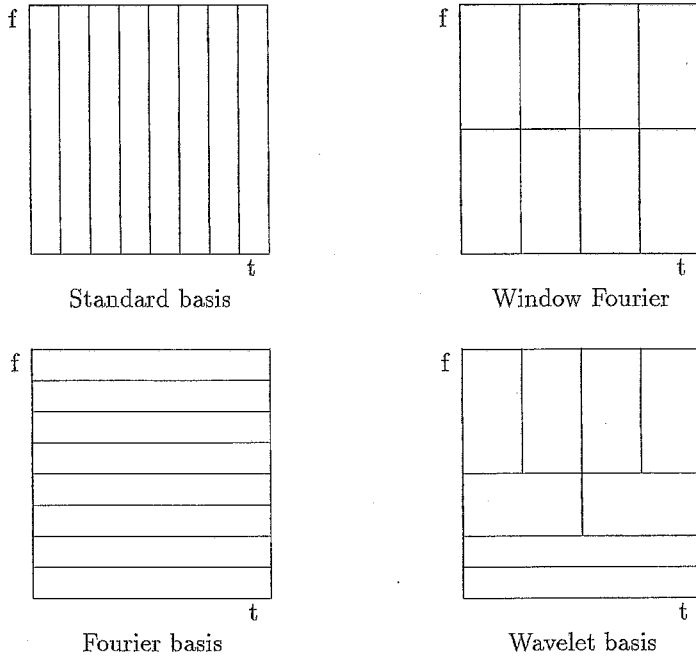


Figure 2.4: Schematic of time-frequency plane decomposition using different bases.

and  $\hat{\psi}(\omega)$  is the Fourier transform of the wavelet  $\psi_{\lambda,b}(t)$ .

The discretization of the scale parameter  $\lambda$  and translation parameter  $b$  leads to the discrete wavelet transform. The choice  $\lambda = 2^m$  and  $b = n2^m$ , results in an orthonormal representation (Daubechies 1988). Mallat (1989a, 1989b) proved that this representation could be simplified by transforming it into what he called the multiresolution framework. This involved the construction of a function  $\phi_{\lambda,b}$  which was given the name *scaling function*. This framework can be easily visualized from a filtering viewpoint wherein the convolution of the signal with the scaling function can be seen as a low-pass filtering and the convolution with the wavelet can be seen as a high-pass filtering. A wavelet decomposition can be seen as a repeated convolution of the low-pass output with two sets of coefficients  $\{c_k\}$  and  $\{d_k\}$ , representing convolution with the scaling function and the wavelet, respectively. From a time-frequency point of view, each stage of the decomposition can be visualized as an improvement of frequency resolution (low-frequency bands) in the frequency domain and a corresponding loss of time resolution (owing to Heisenberg's uncertainty principle). This is illustrated in Figure 2.5.

In the wavelet decomposition case, only the low-frequency bands are decomposed at every stage. Moreover, once the wavelet is chosen, the basis is predetermined. In other words, the basis obtained is not a data-adaptive basis and this may be a restrictive feature. So the idea then is to try and find a framework which can enable us to obtain a data-adaptive basis. Towards this end, Coifman *et al.* (1992) go a step further and obtain a more generic representation by decomposing the high-frequency bands also. The interesting aspect is that, by using a combination of  $\{c_k\}$  and  $\{d_k\}$  to produce 2-scale relations with  $\psi$ , the wavelet spaces,  $W_n$ , can be further decomposed orthogonally. The sequence of functions thus obtained are called "*wavelet packets*". A wavelet packet is defined as a square integrable modulated waveform, well localized in both position and frequency (Wickerhauser 1991). A wavelet packet family can be parameterized by three parameters  $(t, \omega, \lambda)$  where  $t$ ,  $\omega$  and  $\lambda$  are the position of the center of the basis function, the characteristic frequency of the basis function and the characteristic width of the spatial support of the basis function, respectively. It is important to note here that the parameters  $\lambda$  (scale) and  $\omega$  (frequency) are *not* coupled as in a wavelet transform framework. In fact, in a wavelet transform, scale = (frequency)<sup>-1</sup>, i.e., each scale is spanned by a one-period wave. On the other hand, in a wavelet packet framework scale  $\neq$  (frequency)<sup>-1</sup>, i.e., each scale can be spanned by multiple period waves (one-period to Nyquist-period waves).

The total number of levels of decomposition is  $\log_2(N)$  where  $N$  is the signal length. A subset of  $N$  coefficients which correspond to an orthonormal

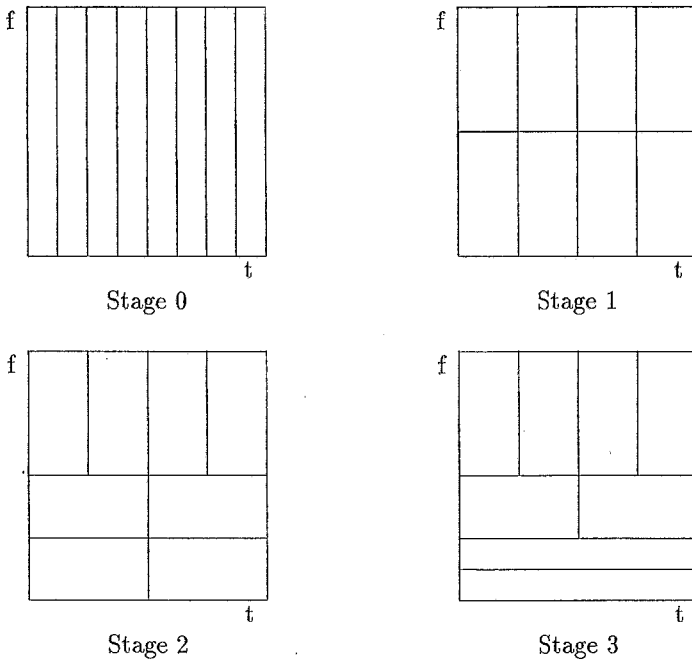


Figure 2.5: Various stages of partitioning of the time-frequency plane in a wavelet decomposition. Note that at every stage the high frequency bands remain intact and the lower frequency bands are further decomposed. Also note that the wavelet basis results in a partitioning of the frequency axis such that it has constant width in the logarithmic scale, or  $\Delta f/f = \text{constant}$ .

basis could be selected and each choice gives a particular basis. The important thing to be noticed here is that a wavelet basis is just one of the ways of choosing this subset. Choosing elements from a single level is analogous to a short-time Fourier transform. The last-level selection, results in a basis analogous to the Fourier basis and the zero-level selection is similar to the standard basis (superposition of *Dirac deltas*).

Thus we have a huge library of orthonormal bases (denoted by  $L$  for further reference), each capable of representing a signal in its own right. Two popular algorithms to extract the best representation out of this library  $L$  have been developed namely, (a) entropy minimization (Wickerhauser 1991) and (b) matching pursuit (Mallat and Zhang 1993). The motivation behind both algorithms is to try and achieve “maximal” contrast between low and high energies which further results in capturing most of the signal’s energy in the least possible number of coefficients.

In the Entropy Minimization algorithm, minimizing entropy results in maximizing information since entropy = - information (see Shannon’s collected papers 1993). The Shannon-Weaver entropy of a sequence  $x = \{x_j\}$  is defined as  $\mathcal{H}(x) = -\sum_j p_j \log p_j$  if  $p_j \neq 0$  and  $= 0$  if  $p_j = 0$ , where  $p_j = |x_j|^2 / \|x\|^2$ . A known aspect about this cost function is that  $\exp \mathcal{H}(x)$  is proportional to the number of coefficients needed to represent the function to a fixed mean square error. The basis so obtained by minimizing entropy is given the name *best basis*. Details of this algorithm can be found in Wickerhauser (1991). In the Matching Pursuit algorithm introduced by Mallat and Zhang (1993) a different procedure to optimally choose a basis out of the library  $L$  is proposed. Optimality is achieved through successive approximations of a function  $f$  with orthogonal projection on elements of  $L$ . The details of the method can be found in Mallat and Zhang (1993).

### 2.2.3 Review of some recent findings for rainfall

#### Simple scaling, multiscaling and multiplicative cascades

The study of Olsson *et al.* (1993) used six one-minute rainfall time series from Sweden (over a period of two years), and determined  $D(0)$  and  $D(2)$  by mass-exponent methods (for  $D(0)$  they used a box-assisted algorithm). They found two definite scaling regions, one for time scales less than the average storm duration and one for time scales greater than the average interstorm period with  $D(0)$  equal to 0.82 and 1.00, respectively (e.g., see Figures 3 and 5 in Olsson *et al.* 1993). They also claimed to have found scaling in the transitional interval, with a  $D(0)$  value of 0.37. Their findings for  $D(2)$  were 0.36 for the transitional interval and 0.84 for scales greater than the interstorm pe-

riod; for scales below the average storm duration they found no scaling in the correlation integral. For a monoscaling measure the values of  $D(0)$  and  $D(2)$  should coincide theoretically. Thus, while the above results do not exclude the hypothesis of monofractality, a multifractal behavior – confirmed by a multifractal analysis presented in the second part of Olsson *et al.* – is most likely the case. However, more data analysis is needed to establish the validity of monofractal scaling in different scale regions versus the alternative hypotheses of either lack of scaling or multifractal scaling in any of these regions. Also, studies with data from different storm types are needed to investigate whether presence of scaling, scaling regions and values of scaling exponents are related to the physical parameters of the storm environment.

Along these lines, a recent study by Svensson *et al.* (1996) compared daily rainfall series from a temperate climate (Sweden) and a monsoon climate (China), and claimed good scaling, specifically multifractal, in the range from one day to one month. The monsoon climate time series showed a higher degree of multifractality (curvature of  $\tau(q)$ ) than their temperate-climate counterparts. In the range of scales greater than one month, trivial scaling associated with a white-noise (flat) power spectrum was reported. In a similar study, Harris *et al.* (1996) reported evidence that the parameters of multifractal cascade models of rainfall are related to orographic influences and specifically that they vary systematically as a function of altitude along a transect.

Within the interval of one storm duration itself, Georgakakos *et al.* (1994) and Cârsteanu *et al.* (1993), performed a fine-scale analysis on 5-s temporal rainfall data of seven storm events from Iowa City, recorded during 1990-1991. A linear decay of the frequency spectra of all seven events was presented as an indication of scale-invariance over short time-scales (at least up to the one-minute range). Also, hyperbolic probability distributions of rainfall intensities and differenced intensities in four of the seven events hinted to a Lévy-type distribution of values in the rainfall process and its differenced version. Multifractal analysis was inconclusive in the study of Georgakakos *et al.*, but later Cârsteanu and Foufoula-Georgiou (1995, 1996) provided evidence of good multiscaling, however with different degrees of multifractality, for all seven events. The log-fits of equation (2.6) showed in all cases high correlation coefficients (see bottom plot in Figure 2.6 for one such case) leading to the conclusion that multiplicative cascades would make good scaling models for those rainfalls. This conclusion was also reinforced by the nondegenerate  $f(\alpha)$  curves, of which an example is shown in Figure 2.6 (middle plot).

A multiplicative cascade model was proposed in Cârsteanu and Foufoula-Georgiou (1996), and a methodology based on “oscillation coefficients” (measuring the occurrence frequency of up-down patterns in the signal) was in-



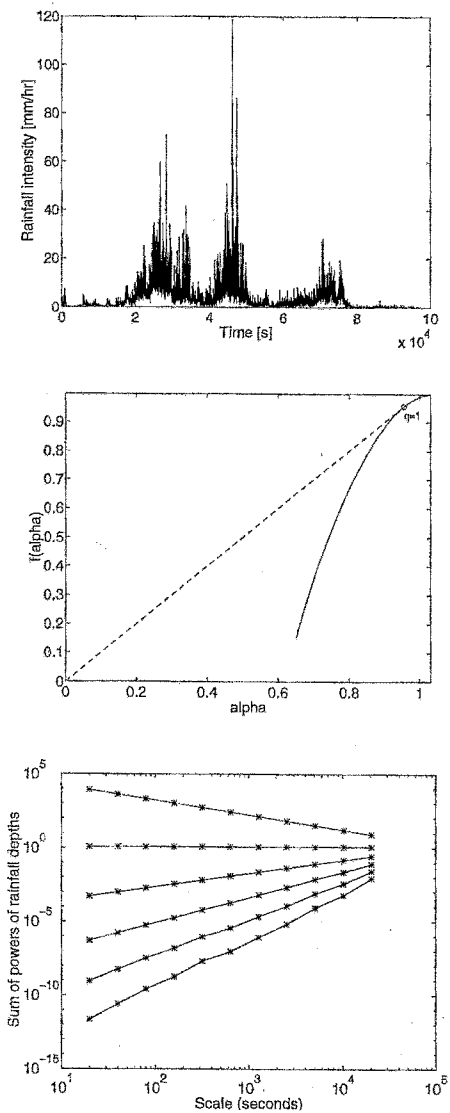


Figure 2.6: (top) The time series of the Iowa City rainfall event of December 2, 1990; (middle) the  $f(\alpha)$  curve for that event; (bottom) log-log fits of  $\sum_t \mu_t^q(\lambda\Delta t)$ , where  $\mu_t(\lambda\Delta t)$  is the rainfall depth over the interval  $(t, t + \lambda\Delta t)$ , against scale  $\lambda\Delta t$  for the same event and for moment order  $q = 0, 1, 2, 3, 4, 5$  (top to bottom). The good log-log linearity of the curves in the bottom plot and the non-degeneracy of the  $f(\alpha)$  curve in the middle plot point towards the presence of multifractality in this rainfall series.

troduced to determine whether a correlation structure in the weights of the cascade model generator is needed to better capture essential statistics of the rainfall process, compared to a cascade model with independent weights. It was found both directly from the rainfall series (under the assumption of complementary, i.e., adding to 1, weights) and based on the oscillation coefficients that a negative dependence structure in the weights of a cascade generator yields an improved representation of the rainfall process. The methodology for arriving at this conclusion is, briefly, as follows.

The oscillation coefficient  $C_{\updownarrow} \equiv C_{\downarrow\uparrow} + C_{\uparrow\downarrow}$ , where  $C_{\uparrow\downarrow} = P[(r_{k-1} < r_k) \wedge (r_k > r_{k+1})]$  ( $r_k$  being the rainfall intensity at time  $t_k$ ) and  $C_{\downarrow\uparrow}$  defined similarly, was introduced as a measure of the stochastic dependence structure of a rainfall series.  $C_{\updownarrow}$  was chosen because it is defined for most cascades, is scale-invariant for multiplicative cascades, and is independent of the underlying probability density function of the cascade generator. Then, a relationship between  $C_{\updownarrow}$  and  $\rho_w(2)$ , the lag-2 autocorrelation of weights, which measures the dependence between consecutive pairs of weights at each level of the cascade generator, was developed. This relationship, shown in Figure 2.7, was found to be independent of the distribution of weights, a one-to-one and linearly increasing function. From Figure 2.7 it is observed that the range of values of  $C_{\updownarrow}$  estimated from the seven rainfall series (values between 0.4 and 0.54) correspond to a region of high negative correlation in the weights of the cascade generator. This negative dependence structure in the cascade generating process of rainfall is in agreement with the hypothesis of anticorrelated (spinning in opposite directions) atmospheric adjacent turbulent eddies and needs to be further explored. Also, some further issues that remain unexplored in this area of research are: (1) development of multiplicative cascade models of rain which preserve the temporal correlation structure of the series at each scale and also the correlation from scale to scale; (2) solution of the inverse problem, i.e., based on observed rainfall series at a particular scale, how can one infer the nature and estimate the parameters of the correlation structure of the cascade rainfall model generator; and (3) understanding of how the correlation structure of the cascade generator relates to atmospheric convectivity or turbulence parameters of the storm environment within which a particular storm is generated.

The issue of scaling within a storm duration was also investigated by Veneziano *et al.* (1996). Using the same seven high-resolution Iowa City series they reported a segmented frequency spectrum of the logarithms of the series. From the slopes of the spectra they concluded that a “bare” (not integrated over its support) cascade model (“multifractal model” in the terminology of the authors) is not appropriate for these events. They proposed an exponenti-

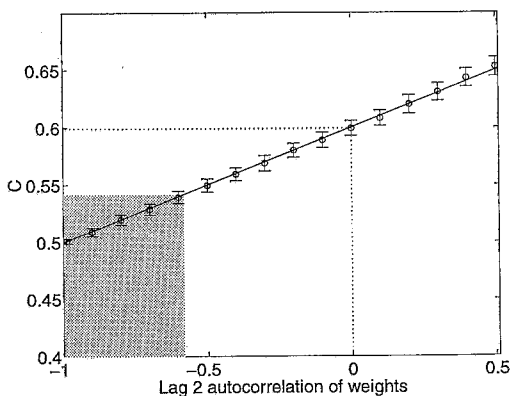


Figure 2.7:  $C_+$  versus lag 2 autocorrelation coefficient of weights  $\rho_w(2)$  in a binary multiplicative cascade. The shaded area corresponds to the region of oscillation coefficients found from the seven analyzed high-resolution temporal rainfall series. For a cascade generator with independent weights ( $\rho_w(2) = 0$ ) the  $C_+$  value was found equal to 0.6 by simulation (dotted line). The error bars are shown for simulations with lognormally distributed weights, but the linear relationship itself was found to be independent of the weight distribution.

ated Brownian motion model. This model is interesting from the perspective of offering an alternative to multiplicative cascades for temporal rainfall, by satisfying causality (present values depend only on the past) and having a different autocorrelation structure than the cascades, possibly closer to the one of the process. However, these issues need to be further explored both theoretically and empirically in reference also to the desire to offer simple rainfall parameterizations rather than overfitting ones at the expense of even not preserving well some rainfall statistics.

In a more recent study, Menabde *et al.* (1997) motivated by a rainfall power spectrum exponent  $|\beta| > 1$ , proposed a cascade with variable parameters over scales, similar to that of Cahalan (1990). The basis of their model is the  $\alpha$  - model of Schertzer and Lovejoy (1983) for which they change the generator parameters such that the cascade becomes smoother at smaller scales.

It is emphasized that the issue of what is the purpose of rainfall modeling should always be kept in mind, as it is different to develop a model for simulation purposes, and different to develop it for inferences about the underlying physical mechanisms giving rise to the observed structures. This is an issue that has not been carefully addressed, and probably causes a good deal of confusion when models are compared or inferences about the presence of scaling or not, are made.

### Time-frequency-scale analysis

Another avenue of exploring the structure of temporal rainfall series is based on the identification of patterns (scale-invariant or not) in the time-frequency plane representation of a process. Based on these ideas, Venugopal (1995) and Venugopal and Foufoula-Georgiou (1996) presented a time-frequency analysis of the Iowa City high-resolution temporal rainfall series. They used wavelet packets to study the energy distribution of rainfall over time, frequency and scale in an effort to gain more insight into the rainfall generating mechanism. In particular, using the seven high-resolution temporal rainfall series from Iowa City, they investigated the existence of persistent and short-lived structures and their associated frequencies and time scales, as well as the energy they carry. They then conjectured that the high-energy short-lived structures of high-frequency may be associated to the convective portion of the rainfall event and the low energy persistent structures of high or low frequency, to the stratiform portion. Separation of the convective and stratiform portions of a rainfall event is important, especially for spatial rainfall since their different three-dimensional structures affect cloud parameterizations in atmospheric models as well as the energy and heat balance calculations over a storm do-

main.

In Venugopal and Foufoula-Georgiou (1996) it was postulated that the different vertical small-scale motion structures within convective and stratiform clouds would leave their signatures in the frequency-content and length scales of identifiable entities or “atoms” from which the rainfall process is composed. Also, it was postulated that the time-frequency decomposition would provide information which can be used to infer the “rules” of energy splitting in a cascade model of rainfall. Although a type of energy branching is apparent in the time-frequency decomposition of a rainfall series (e.g., see Figure 2.8), it is not clear how one can use this information to directly infer the structure of a branching or cascading model for the rainfall process. It can be shown, for example, that the structure of a cascade leaves a clear signature on the time-frequency plot but the inverse problem is not trivial. Figure 2.9 shows the time-frequency plots (using a Mexican hat wavelet) of (a) a ternary Cantor set with weights  $p_1 = 1/2$ ,  $p_2 = 0$ , and  $p_3 = 1/2$ ; (b) a deterministic cascade with  $p_1 = 1/3$ ,  $p_2 = 2/3$ ; (c) a random cascade with  $p_1 = 1/3$ ,  $p_2 = 2/3$ . A few things can be noted from Figure 2.9.

First, in Figure 2.9a the construction rule of the underlying Cantor set is clearly apparent and the logs of the vertical distances between branchings are constant, as is theoretically expected. Second, in Figure 2.9b the concentration of dark (high energy) at the left and right edges of the plot should be ignored, as it is due to end effects caused by periodic convolution. Apart from that, it is observed that the branching of the underlying cascade is fairly clear and it occurs at vertical distances of constant size in logarithmic scale. The regularity in the order and appearance of maxima (in both magnitude and position) is also apparent. The Wavelet Transform Modulus Maxima (WTMM) technique (e.g. Arnéodo *et al.* 1994) is expected to clearly identify the underlying binary cascade structure and its weights from this time-frequency plot. Third, in Figure 2.9c it is observed that the introduction of randomness in the weights (here a structured randomness, consisting of flipping the order of fixed-value weights in a random way at each iteration) masks many of the features of the underlying cascade generator. Nevertheless, the branching and scaling structure is still clearly visible. Obviously, more rigorous analysis of these plots is needed to understand how the known cascading structure of the underlying signals manifests itself in the time-frequency domain so that the inverse problem can be attempted with confidence.

One problem of particular interest is the determination from the plot of Figure 2.8 of the structure of an energy cascading model for rain, e.g., whether it is dyadic or triadic, if it is uniformly cascading over its whole energy domain or over some of the domain only and whether a dependence structure in the

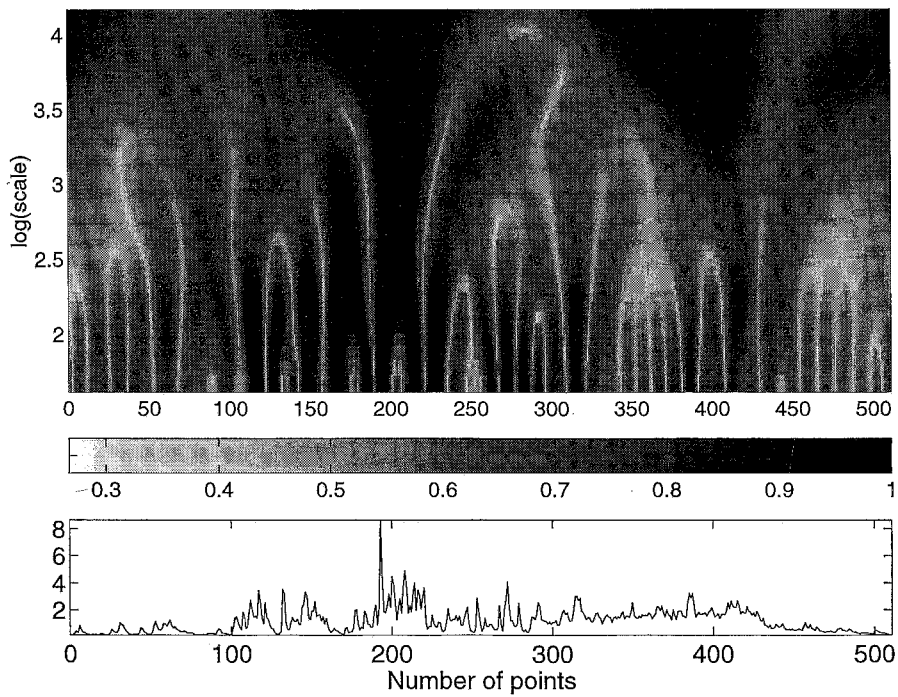


Figure 2.8: Analysis of the high resolution Iowa City rainfall event of Nov 30, 1990, using a Mexican Hat wavelet.

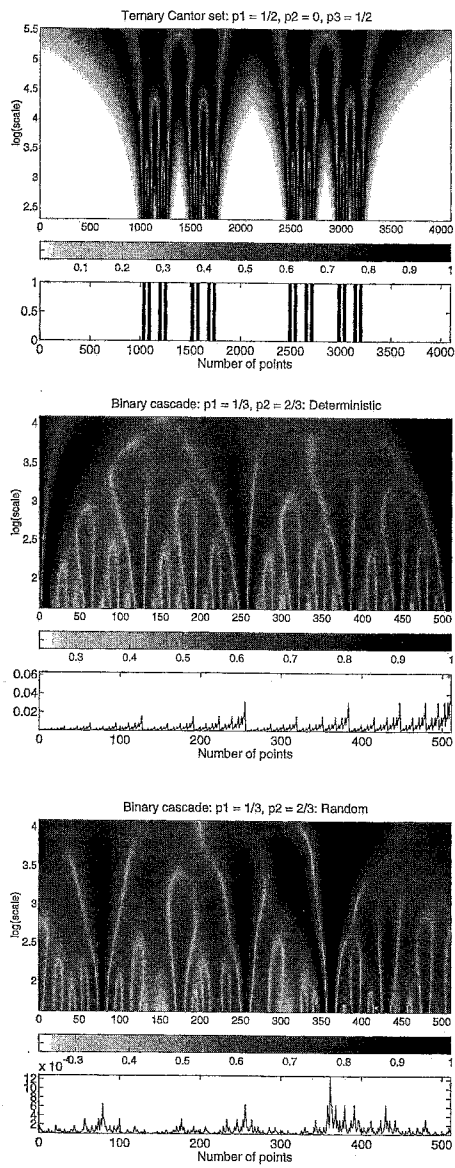


Figure 2.9: Analysis of multiplicative cascades using a Mexican Hat wavelet. (a) Ternary Cantor set with weights  $p_1 = 1/2, p_2 = 0, p_3 = 1/2$ ; (b) Deterministic binary cascade with  $p_1 = 1/3, p_2 = 2/3$ ; and (c) Random binary cascade with  $p_1 = 1/3, p_2 = 2/3$

cascading mechanism is present or not. Recent studies in turbulence using wavelet packets (e.g., Fargé *et al.* 1992, 1996; and Wickerhauser *et al.* 1994) suggest that cascading of energy in turbulent flows takes place only locally within coherent structures (defined as local condensations of the vorticity field which survive for times much longer than the eddy turnover time). They also find that only a limited active portion of the vorticity field, related to coherent structures, is responsible for the turbulent cascades. This is against the assumptions of previous cascade models in turbulence, which assumed that wavenumber octaves are the elementary objects and that interactions consist of exchanging energy with neighboring octaves only. Methods based on the work of Arnéodo's group (e.g., Arnéodo *et al.* 1992a, 1992b, 1994) who are developing tools for the solution of the "inverse fractal problem" using wavelets are expected to be very useful and offer an open area for rainfall research in this direction. Arnéodo *et al.* (1994) argue that  $D(q)$  and  $f(\alpha)$  provide only "macroscopic" statistical information about the self-similar properties of fractal objects. Multifractal description is incomplete mainly because, to some extent, the information concerning the hierarchical architecture of these objects has been filtered out. To achieve a more elaborate structural analysis, they advocate the use of the continuous wavelet transform as this is well adapted to the large hierarchy of scales involved in fractal patterns. The premise of their methods is based on the fact that a dynamical system which leaves invariant a fractal object can be uncovered from the space-scale arrangement of its wavelet transform, given a general expression for the system. Arnéodo *et al.* (1994) demonstrates this methodology by uncovering (i.e., providing statistical evidence for) a multiplicative process hidden in the geometrical complexity of diffusion-limited aggregates. Similar methodologies are developed and discussed in Bacry *et al.* (1993), and Muzy *et al.* (1994).

Using the time-frequency-scale decomposition obtained via wavelet packets and the matching pursuit algorithm, Kumar (1996) attempted to identify the coherent structures that can capture the essential dynamics of the precipitation process. It was argued that when the original function correlates well with a few dictionary elements (i.e., elements of the library  $L$  of orthonormal bases discussed in the previous section), these correlated components represented "coherent structures" (Davis 1994), and the remaining portion was called residue or noise with respect to the chosen dictionary. It is noted that although the term "coherent structure" as used in that study is not strictly in accordance with that used in the turbulence literature, it is not inconsistent with that notion, either. In turbulence the term is used to describe a region of flow over which at least one fundamental flow variable (vorticity, velocity, density, temperature, etc.) exhibits significant correlation with itself or with another



variable (Robinson 1991). Kumar (1996) used the term coherent structure to describe regions where the variable under study is significantly correlated with the basis elements, and these regions will have meaningful characteristics, provided the basis elements have meaningful properties. The choice of wavelet packets as basis elements enables one to identify fluctuations that persist or have a lifetime greater than their characteristic wavelength. Kumar (1996) applied the method to the seven high-resolution temporal rainfall sequences from Iowa and argued for the presence of dominant scales of variation in rainfall. In particular, he found that while the best basis picked up approximately 40 coefficients from each of levels 8 and 9, high energy (approximately 40% of the total energy of the signal) was concentrated at level 9 of the decomposition, which corresponded to scales of approximately 40 mins, while the energy from level 8 (which corresponded to scales of approximately 20 mins) was negligible (see Figure 2.10). This result tempts one to attach special meaning to the scale of level 9 and consider it a distinct scale of variation.

It is reminded that in that analysis the “activity” at every level was identified from its representation within a best basis. However, the contribution of each level to the best basis does not necessarily reflect the activity contrast within the level itself. That is, the best basis might not pick up the highest coefficient from a particular level but pick up a lower one if that coefficient is found to globally (i.e., over all levels) achieve the highest energy contrast. Our preliminary results suggest that the highest 40 wavelet packet (not best basis) coefficients from level 7 carry almost the same energy as the 40 highest coefficients from level 8, or level 9, or level 10 for the Iowa City rainfall series (e.g., see Figure 2.11 for the Dec 2, 1990 series). Moreover the best basis curve falls close to all these curves. The energy curves for levels greater than 7 (scales greater than approximately 20 mins) almost collapse into a single curve while lower levels show a distinct pattern in their energy recovery. Whether or not this behavior indicates a break in scaling and distinct scales of variation is a question that needs further investigation and is expected to lead to useful inferences about the underlying structure of rainfall.

#### *2.2.4 Where do we stand?*

From the discussion in the previous section it is clear that a lot of new ideas have emerged and have been explored in the past five years or so towards a better understanding of the temporal rainfall structure. Most of these ideas have as underlying premise the strong desire to unravel scale invariances in rainfall, at least within a range of scales, for the purpose of either parsimonious modeling, or for physical inferences on the rainfall process. It is repeated that while

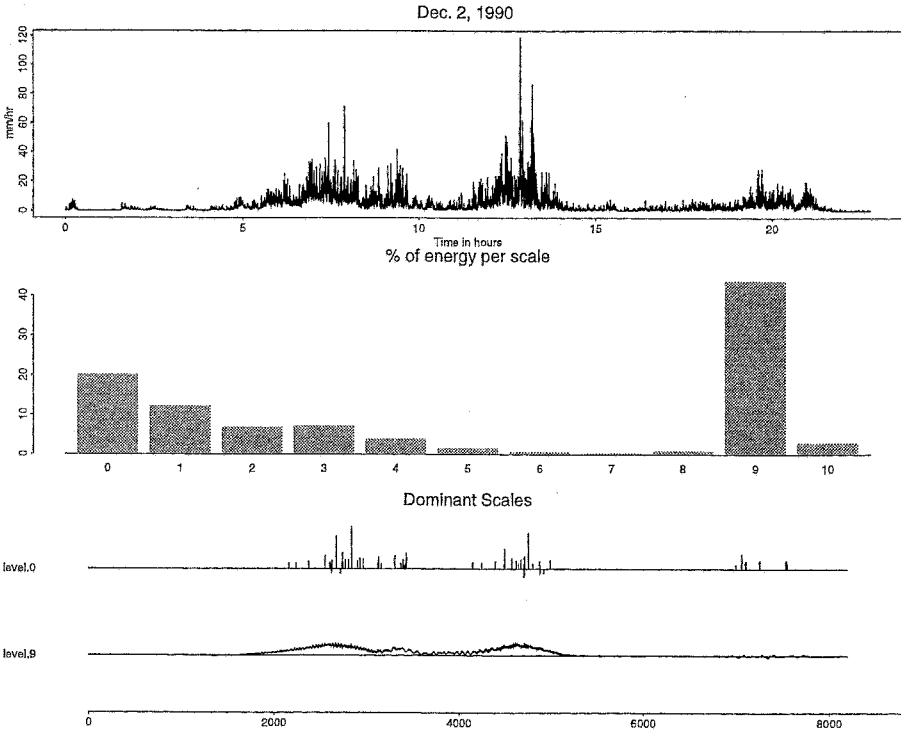


Figure 2.10: (Top) Rainfall time series observed at a point in Iowa City on December 2, 1990. The data is available at 10 second sampling interval and consists of 8192 points. (Middle) Energy at different scales obtained using a wavelet packet decomposition with matching pursuits algorithm. Notice the peaks in energy at levels 0 and 9. (Bottom) Reconstruction of the rainfall series using the best basis coefficients only from level 0 and level 9 (from Kumar and Foufoula-Georgiou 1997).

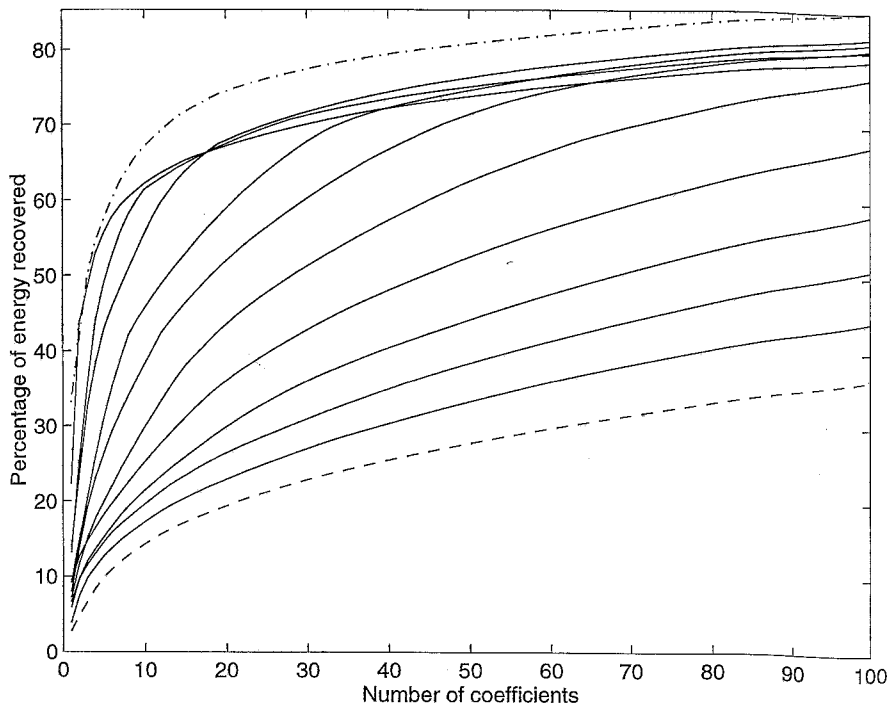


Figure 2.11: Percentage of recovered energy as a function of the number of highest wavelet packet coefficients from each level needed to recover that energy. This figure is for the Iowa City rainfall time series of December 2, 1990 as presented in Figure 2.6. The signal (level 0 in the wavelet packet tree) is represented in dashed line, the levels 1 to 10 in continuous line, and the best basis in dash-dotted line.

a reasonable approximation with a scaling structure for the purpose of modeling and simulation might be acceptable, one has to be more cautious about physical inferences resulting from the same approximations. The reason is that physical inferences should more or less be absolute and not highly dependent on our methods of questioning, while a model for generation may always be conditioned on the properties it is meant to describe best, acknowledging less ability to capture some other properties.

Our discussion was centered on relatively new efforts to unravel scaling or underlying predominant features in the rainfall process. Obviously, no consensus has yet been reached on the presence and type of scaling present in high-resolution temporal rainfall. As the ideas and methodologies mature, it is natural that they will integrate to a clearer picture about the underlying structure of the rainfall process and its generating mechanism. We believe that these efforts will greatly benefit from new mathematical developments in time-frequency-scale analysis and fractal analysis using wavelets (e.g., see Wornell 1996).

In an excellent paper by Fargé *et al.* (1996), the shortcomings in conceptual and technical tools necessary for understanding turbulence and its unsolved problems are very clearly discussed. It is argued that in fully developed turbulence where nonlinear convection is dominant, i.e., it is larger than linear dissipation by a factor of the order of Reynolds' number  $\mathbf{R}$  (in meteorology of the order of  $10^8$  to  $10^{12}$ ) it is obvious that Fourier representations are inadequate for studying and computing turbulent flows. Thus, a new mathematical tool is needed to optimally solve the nonlinear convective term in the same way as Fourier transform is the most economical representation to solve the linear dissipative term. They argue that this new mathematical tool is offered by wavelets and wavelet packets, which supply new functional bases better adapted to represent and compute turbulent flows, i.e., extract their elementary dynamical entities, perform the appropriate averaging on them and predict the evolution of these statistical quantities. Since rainfall is really a tracer carried inside the turbulent atmospheric fields, it is logical that statistical theories of turbulence have heavily influenced statistical theories of rainfall. However, we feel that apart from the introduction of multifractal rain models based on the turbulence cascade models, new advances in turbulence research have not been adequately explored for rainfall research. This leaves an open opportunity for further advances on understanding this complex phenomenon.

Rainfall is a prime example of a process where a good model is difficult to be established based on first principles. Thus models must be found directly from the data. It is a well known fact that apparent randomness in a time series may be due to chaotic behavior of a nonlinear but deterministic system.

Thus chaos provides a link between deterministic systems and random processes, with both good and bad implications for prediction. In a deterministic system, chaotic dynamics can amplify small differences which in the long run produces effectively unpredictable behavior (even approximate long-term predictions may be impossible). On the other hand, chaos implies that not all random looking behavior is the product of complicated physics; it is possible to model this behavior deterministically and make short-term predictions far better than those obtained from linear stochastic models.

Thus, in parallel to scaling research, we believe that nonlinear modeling of temporal rainfall as a dynamical system should also be pursued. The first attempt along this direction was made by Rodriguez-Iturbe *et al.* (1989), who analyzed phase-space dimensionality of rainfall time series. They concluded that it is possible that the orbits of the rainfall process might live on a low dimensional attractor, which would open the possibility of modeling the process with lesser degrees of freedom than previously believed. Acknowledging that the dynamics of a physical system are never really deterministic due to “dynamical noise” and that observations are never completely accurate due to “observational noise”, the problem of unraveling a low-order deterministic system from the noisy rainfall measurements needs special attention. We believe that not enough effort has been directed towards this line of research and that new methodologies on nonlinear modeling of chaotic time series in the presence of dynamical and observational noise (e.g., Casdagli *et al.* 1995a, 1995b) would be useful.

Finally, the ideas of scaling (simple or multiple) should be studied in conjunction with the ideas of nonlinear dynamics to explore if such a higher level of integration is fruitful or even possible. Rainfall research in this direction offers a unique opportunity for new mathematical developments which will then positively feed back into empirical investigations.

## 2.3 Spatial Rainfall Scaling: Relationships of Statistics and Physics

### 2.3.1 Preliminaries

In parallel to temporal rainfall research, the analysis and modeling of rainfall's spatial structure has also been studied intensively by several researchers. Again, the most recent developments are based on ideas of scale-invariance over a range of scales and several model structures have been proposed (e.g. Schertzer and Lovejoy 1987; Gupta and Waymire 1990, 1993; Tessier *et al.* 1993; Kumar and Foufoula-Georgiou 1993b; see also Foufoula-Georgiou and Krajewski 1995 for a brief review and further references). The purpose of this

section is not to provide an overview of these models but rather focus on a particular aspect of spatial rainfall research: that of trying to relate statistical (scaling) and physical parameterizations of rain. This has been an issue of continuous interest for the purpose of gaining a better understanding of the physics responsible for the observed rainfall structure and for providing the ability to attach physical meaning and interpretation to statistical parameters of rain (see also Over and Gupta 1994, Harris *et al.* 1996, and Lawford, 1996).

In a series of recent papers, an extensive investigation of the statistical spatial structure of several storm types (Kumar and Foufoula-Georgiou 1993a, 1993b) as well as the corresponding thermodynamical parameters of the storm environments (Perica and Foufoula-Georgiou 1996a, 1996b) was reported. We describe here in brief the main premise of this line of research and the main findings of these studies with interpretations, open problems and directions for further research.

### *2.3.2 Scaling in standardized rainfall gradients*

Contrary to most studies which investigate rainfall intensities themselves for the presence of scaling, Kumar and Foufoula-Georgiou (1993a, 1993b) set forth the hypothesis that if spatial rainfall is decomposed in multiscale means and multiscale “fluctuations” (i.e., gradients or generalized differences), the multiscale fluctuations are more likely to obey some simple universality condition like self-similarity than are rainfall intensities themselves. This is because the low frequency components in the rainfall process are mainly related to the storm morphological organization due to the large-scale forcing which is special to that particular rain producing mechanism (for example, effects of a front on a squall line). When these effects are subtracted, the deviations which result from the microscopic or small-scale convection effects are more apt to be exhibiting self-similarity along scales and more apt to be controlled by the convective instability of the storm environment. In other words, the rainfall averages over scales carry in them the signature of deterministic background features making it unlikely to share simple scaling relationships over a significant range. Once, however, these underlying deterministic features are removed, the remaining features (called “local fluctuations”) are more amenable to stochastic parameterizations which might present similarities over a significant range of scales.

To implement and test this hypothesis in spatial rainfall, a methodology based on filtering which could segregate large and small-scale features efficiently and consistently over scales was needed. The filter would have to be “local” to be able to handle nonstationarities, “directional” to be able to han-

dle preferred storm orientations, “multiscale” to be able to simultaneously, consistently and efficiently extract features over several scales, and also “re-constructive” so that the original process could be obtained back from “superposition” of all the multiscale features. Kumar and Foufoula-Georgiou (1993a) proposed the use of orthogonal wavelet transforms for this multiscale decomposition and demonstrated their usefulness for the extraction of “multiscale rainfall fluctuations” from the radar scans of rainfall. Using a separable two-dimensional Haar wavelet (which implies three directions), it was shown that the Haar wavelet coefficients at every scale (and direction) correspond to the rainfall “fluctuations” at that scale (and direction), which were interpreted physically as directional differences or gradients of the rainfall intensity field.

Kumar and Foufoula-Georgiou (1993b) also proposed a rigorous methodology for scaling analysis of the rainfall fluctuations and presented preliminary evidence for the presence of simple-scaling relationships. Later Perica and Foufoula-Georgiou (1996a) presented an extensive analysis of many storms monitored by radar during the Oklahoma-Kansas Preliminary Regional Experiment for Storm-Central (PRESTORM) field program that took place in May and June of 1985 (see Cunnig 1986 for details on that program). They concluded that “standardized rainfall fluctuations”, i.e., rainfall fluctuations divided by the same-scale local means, exhibit Normality and simple scaling. It was also found that directionality in wavelet coefficients was not significant and that for most midlatitude mesoscale convective systems an “average parameterization” of fluctuations in all three directions could result by simply averaging the directional parameters over all directions. The simple scaling was found over scales of  $4 \times 4 \text{ km}^2$  to  $64 \times 64 \text{ km}^2$ . The lower scale of 4 km was imposed by the radar data resolution and the upper scale of 64 km was selected so that enough averaging cells within the radar images were available for a meaningful statistical analysis. The analyzed scales were selected dyadically for computational efficiency in implementation of the discrete orthogonal Haar wavelet transform.

Let us define by  $\xi_L$  the standardized rainfall fluctuations at scale  $L$  obtained as

$$\xi_L = X'_L / \bar{X}_L \quad (2.17)$$

where  $X'_L$  is the rainfall intensity gradient at scale  $L$  (obtained via a multiscale filtering of spatial rainfall intensities with a Haar wavelet) and  $\bar{X}_L$  is the average rainfall intensity at the same scale  $L$  (obtained via filtering with the “scaling function” complementary to the chosen wavelet). The simple scaling of  $\xi_L$  implies that

$$\frac{\sigma_{\xi_L, L_1 \times L_1}}{\sigma_{\xi_L, L_2 \times L_2}} = \left( \frac{L_1}{L_2} \right)^H \quad (2.18)$$

where  $\sigma_{\xi, L_1 \times L_1}$  denotes the standard deviation of  $\xi$  at scale  $L_1$  (kilometers) and  $H$  is a scale-invariant exponent. It is noted from (2.18) that if one knows the value of  $\sigma_{\xi}$  at one particular reference scale and the value of  $H$ ,  $\sigma_{\xi}$  at any other scale can be easily computed. In the work of Perica and Fofoula-Georgiou (1996a), that reference scale was chosen to be the 8 km scale as this was the smallest scale at which wavelet fluctuations were defined. (Note that the smallest scale at which fluctuations via a discrete orthogonal wavelet transform are defined, is one dyadic scale larger than the observation scale, which was 4 km in our case). Once the parameters  $H$  and  $\sigma_{\xi, 8 \times 8}$  are known, statistical reconstruction of the small-scale rainfall variability, given a large-scale rainfall average can be obtained through an Inverse Wavelet Transform (IWT) since wavelet is a reconstructive filter. The question then was asked whether the parameters  $\sigma_{\xi, 8 \times 8}$  and  $H$  can be predicted from physical observables of the storm environment. Before these findings are reviewed a mention is made as to the relation of the Normality and simple scaling in standardized rainfall fluctuations found by Perica and Fofoula-Georgiou (1996a) to other developments of rainfall geared more towards multiplicative and multifractal models.

While theoretically the connections between wavelets and multifractals have been made by Arnéodo *et al.* (1993), Veneziano *et al.* (1996) have made some important specific observations which point out to the consistency of simple scaling in standardized rainfall fluctuations with a multiplicative-type structure for rainfall, as found by them and other authors. Simply put, it is sufficient to notice that since  $d(\ln X) = dX/X$ , the approximation

$$\Delta X/\bar{X} \approx \Delta(\ln X) \quad (2.19)$$

holds. This implies that scaling in  $\Delta X/\bar{X}$  (equivalent to the Haar standardized wavelet coefficients  $\xi = X'/\bar{X}$ ) is same as scaling in the differences of the logs of rain, at least for small values of  $\Delta X$  for which the above approximation holds. Thus simple scaling in standardized rainfall fluctuations found by Perica and Fofoula-Georgiou (1996a) is consistent with the exponentiated Brownian motion (Bm) model proposed by Veneziano *et al.* (1996). Also, normality in  $\Delta X/\bar{X}$  implies, within the approximation (2.19), Normality of the logs of rain which is again consistent with the exponentiated Bm model.

Veneziano *et al.* (1996) expressed concern about the assumption of Perica and Fofoula-Georgiou (1996a) that standardized rainfall fluctuations can be approximated with a Normal distribution at all scales. They argued that Normality in standardized rainfall fluctuations (which lie by definition in the interval  $[-1, 1]$ ) cannot be preserved over a large range of scales due to the increasing variance of the respective Normal distributions. Nevertheless, the



data showed that at the largest scales analyzed, the distributions of standardized fluctuations (in the overwhelming majority of cases) were narrow enough to warrant Normal approximations almost completely contained within  $[-1,1]$ .

### 2.3.3 Relation of scaling parameters to physical observables

A particularly useful and informative parameter of the atmospheric dynamics in a storm environment is the amount of buoyant energy available to a parcel of air rising vertically through an undisturbed environment from the level of free convection (LFC) to the equilibrium level (EL). The LFC is the height at which a parcel of air lifted dry-adiabatically until saturated and wet-adiabatically thereafter would first become less dense than the surrounding air, and the EL is the lowest level of zero potential temperature excess above the LFC. This buoyant energy is called convective available potential energy (*CAPE*) and is a measure of the potential instability at the middle and upper levels of the atmosphere. *CAPE* at a point is defined as:

$$CAPE = A \int_{LFC}^{EL} (T_{sa} - T) d\tilde{p} \quad (2.20)$$

where  $T$  is temperature,  $\tilde{p} = (P/P_o)^{0.286}$  with  $P$  being pressure and  $P_o$  reference pressure (1000mb),  $A = -4186.8 \text{ m}^2 \text{ s}^{-2} \text{ K}^{-1}$  is unit converting factor (the negativeness of  $A$  is due to the fact that the pressure at *LFC* is greater than that at *EL*) and  $T_{sa}$  is the saturated adiabat crossing the lifted condensation level (*LCCL*), to which a parcel of air from the lowest 500 m of the atmosphere rises dry-adiabatically until saturated.  $T$ ,  $\tilde{p}$ , and  $T_{sa}$  are functions of vertical levels (or height) (Air Weather Service 1979).

Perica and Foufoula-Georgiou (1996a) found that for midlatitude mesoscale convective systems,  $H$  and  $\sigma_{\xi,8 \times 8}$  are related to the convective available potential energy (*CAPE*) in the prestorm environment by the following empirical relationships:

$$H = 0.0516 + 0.9646 \text{ CAPE} \times 10^{-4} \quad (2.21)$$

$$\sigma_{\xi,8 \times 8} = 0.5390 - 0.8526 \text{ CAPE} \times 10^{-4} \quad (2.22)$$

where *CAPE* is in  $\text{m}^2 \text{ s}^{-2}$  and  $H$  and  $\sigma_{\xi,8 \times 8}$  are dimensionless (see also Figure 2.12). Eqs. (2.21) and (2.22) led for the first time in establishing empirical relationships between statistical scaling and thermodynamic parameters of storms.

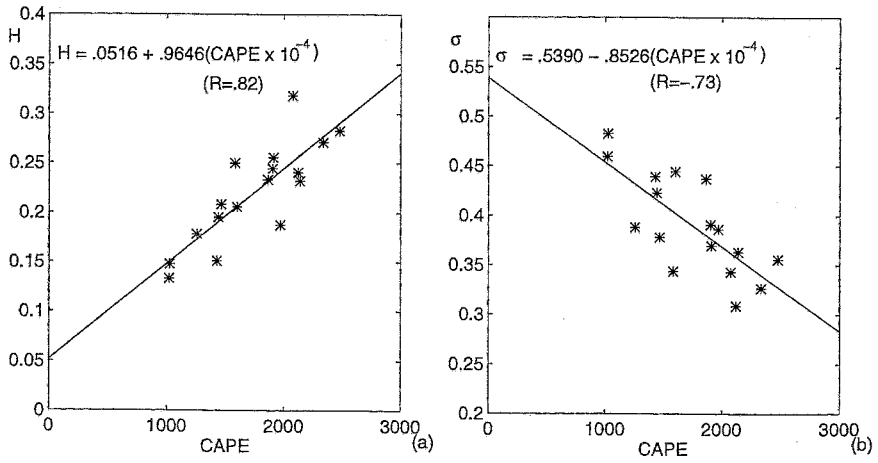


Figure 2.12: Scattergrams with indicated regression lines and correlation coefficients of (a) convective available potential energy (CAPE) and  $H$ ; (b) CAPE and  $\sigma_{\xi,8 \times 8}$ . The units of CAPE are  $\text{m}^2/\text{s}^2$ .

Based on the above developments, a new physical/statistical scheme for multiscale rainfall disaggregation (downscaling) was developed by Perica and Foufoula-Georgiou (1996b). This scheme uses an Inverse Wavelet Transform (IWT) to obtain rainfall intensities at any scale smaller than the initial scale (e.g., from  $64 \times 64 \text{ km}^2$  averages down to  $4 \times 4 \text{ km}^2$  averages in that study). Briefly, the downscaling scheme is implemented as follows: once  $CAPE$  is known,  $H$  and  $\sigma_{\xi, 8 \times 8}$  are computed from eqs. (2.21) and (2.22). Then, standardized rain fluctuations at any other scale  $L$  are generated from a Gaussian distribution with zero mean and standard deviation  $\sigma_{\xi, L \times L}$  computed from eq. (2.18) using the known values of  $\sigma_{\xi, 8 \times 8}$ , and  $H$ . These fluctuations are then randomly distributed in space over grid boxes at scale  $L \times L$  and are multiplied by the corresponding rainfall average values at that same scale. Then they are “added” via an inverse wavelet transform (IWT), to these averages to get rainfall intensities at the next finer scale. This procedure is repeated at all intermediate scales down to the finest scale of interest. Fig. 2.13 shows one example where the IWT model was used to downscale rainfall from  $64 \times 64 \text{ km}^2$  average down to  $4 \times 4 \text{ km}^2$  averages. It is seen that the disaggregated (simulated) fields at all intermediate scales compare well to the actual fields. More details and a formal statistical comparison can be found in Perica and Foufoula-Georgiou (1996b).

#### 2.3.4 *Coupling of atmospheric models with statistical scaling rainfall descriptions*

Despite great advancements in atmospheric modeling research, rainfall still remains one of the most difficult variables to predict in numerical weather prediction models. Currently, global circulation models and mesoscale models attempt to resolve rainfall at scales of the order of 100-200 km and 10-30 km, respectively, since it is too expensive and often computationally prohibiting to run high resolution simulations over large areas and over long durations. Thus, the need often arises to resolve the smaller scale rainfall variability in some other statistical way. Redistribution of the large-scale average rainfall intensity value to subgrid scale values is important for two main reasons: (1) to improve the hydrologic predictions at the basin and subbasin scales through distributed rainfall-runoff modeling, and (2) to improve the grid and subgrid scale atmospheric variable predictions due to the feedback effects of rainfall variability through coupled modeling.

This last issue was explored recently by Zhang and Foufoula-Georgiou (1997) by incorporating the statistical/dynamical rainfall downscaling scheme of Perica and Foufoula-Georgiou (1996b) into the Penn State NCAR Mesoscale

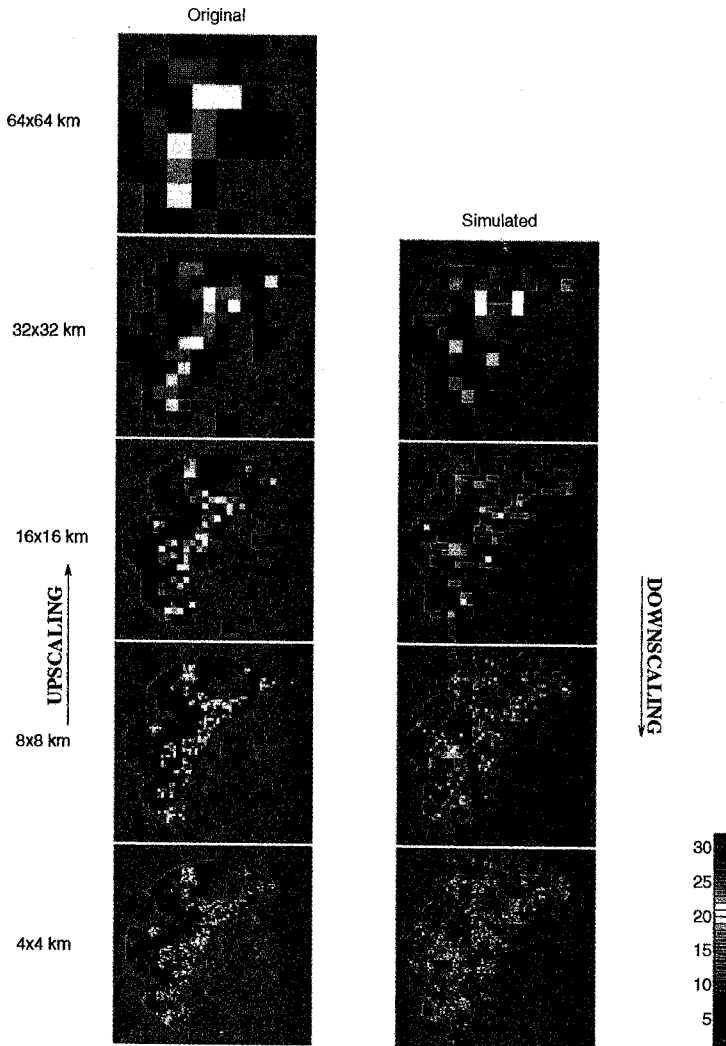


Figure 2.13: The June 27, 1985 storm over Kansas-Oklahoma at 0300 UTC. The bottom figure in the left column shows the original radar data at  $4 \times 4 \text{ km}^2$  resolution. From these data, rainfall fields at lower and lower resolutions were obtained by averaging, up to  $64 \times 64 \text{ km}^2$  averages as shown in the top panel (upscaling). Then, using the  $64 \times 64 \text{ km}^2$  field and the downscaling scheme of Perica and Foufoula-Georgiou (1996b), rainfall fields at higher resolutions were reconstructed down to the resolution of  $4 \times 4 \text{ km}^2$ , as shown in the bottom right panel. A good agreement was found between the rain patterns and the areas covered by rain of the simulated and original fields at all resolutions. A more rigorous quantitative comparison of several statistical measures of the original and simulated fields can be found in Perica and Foufoula-Georgiou (1996).

Model (MM5). MM5 (e.g., see Grell *et al.* 1994) is one of the most widely used state-of-the-art atmospheric modeling systems. It solves the full set of dynamical equations that describe the conservation of mass, momentum and energy in the atmosphere and a set of microphysics equations for different phase clouds and precipitation. It was found in Zhang and Foufoula-Georgiou (1997) that the feedback effects from the subgrid-scale rainfall spatial variability on the further development or short-term (i.e., <24 hrs) numerical prediction of rainfall are significant. For example, Figure 2.14 shows the changes of ground temperature in deg C (colour variation) and rainfall intensity in mm/h (black and white curves) caused by adding the feedback effect of subgrid-scale rainfall variability to the MM5 simulation of the storm of June 11, 1985 at 0600 UTC. The feedback effects were simulated by adjusting, according to the subgrid scale rainfall intensities, the subgrid scale moisture availabilities and soil roughnesses, and the thermal capacity at the MM5 nodes (see Zhang and Foufoula-Georgiou 1997). The temperature (or rainfall) change was measured by the difference between the temperature (or rainfall) fields computed with two runs: the MM5 model run at 12 km resolution and the same run with the 1.5 km resolution rainfall downscaling scheme implemented in a two-way interactive coupling. The comparisons shown in Figure 2.14 are for the 12-km resolution domain.

It is observed that ground temperature changes by up to 5 degrees and that the strongest variation in ground temperature change takes place ahead of the center of the squall line. Also the black and white curves on the figure indicating the increase and decrease of rainfall intensity with peak values of 55.2 mm/h and 66.6 mm/h respectively, demonstrate that the inclusion of the subgrid scale rainfall variability has exerted significant effects on the resolved rainfall development over the MM5 model grids and has contributed to an enhancement of the contribution of the convective component of the total rainfall (see Zhang and Foufoula-Georgiou 1997 for more details). Of course, more research is needed to study the feedback effects of the subgrid scale rainfall variability on the energy and water budget partitioning at the grid and subgrid scales. For example, more sophisticated land-atmosphere interaction schemes within atmospheric models must be used in addressing this question so that more confidence is gained that the changes we see are mostly due to the inclusion of the subgrid rainfall variability and not due to inadequate handling of the land-atmosphere feedback effects. The practical implications of improving atmospheric and hydrologic predictions efficiently and cost-effectively using statistical redistribution of subgrid scale rainfall or improved convective rainfall parameterizations, rather than very high resolution coupled modeling requiring supercomputers, is exciting and provides sufficient motivation for further

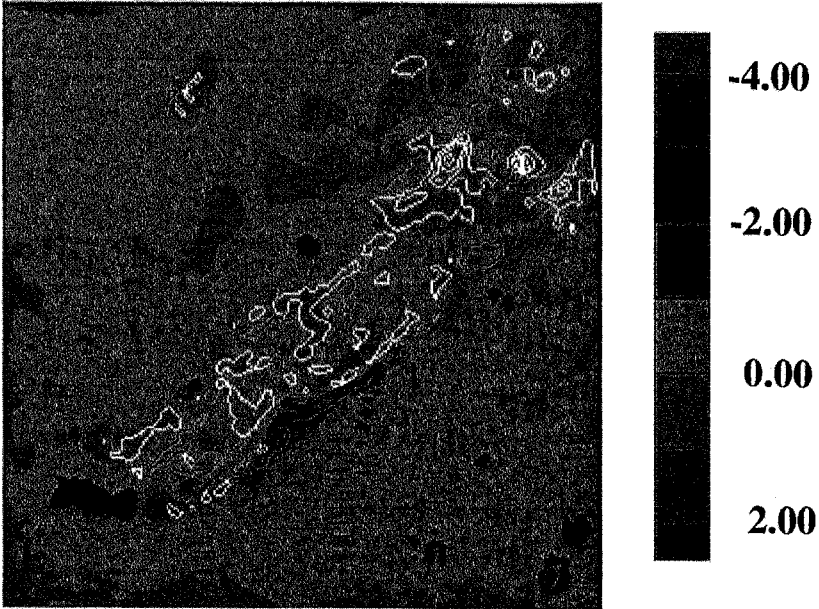


Figure 2.14: Changes in ground temperature in  $^{\circ}C$  (color variation) and rainfall intensity in mm/h (black and white curves) caused by adding the feedback effect of subgrid-scale rainfall variability to the simulation of the June 11, 1985 storm using the MM5 model with two nested domains of 36 km and 12 km, respectively. The comparison (differences in values between the run without and with subgrid scale parameterizations) is shown for the domain of 12-km resolution. The black and white curves indicate the increase and decrease of rainfall intensity with peak values of 55.2 mm/h and 66.6 mm/h, respectively. For more details, see Zhang and Foufoula-Georgiou (1997).

research along this direction.

### 2.3.5 Discussion and some open problems for further research

The statistical subgrid scale parameterization scheme of Perica and Foufoula-Georgiou (1996b) offers in itself great advantages over many currently used approaches (e.g., see Schaake *et al.* 1996, Warrilow *et al.* 1986, and the review article of Thomas and Henderson-Sellers 1991). First, it is dynamical in the sense that its parameters ( $\sigma_{\xi, 8 \times 8}$  and  $H$ ) are updated as the storm evolves based on the evolution of the convective instability of the storm environment measured by CAPE. Second, its parameterization is scale-independent within a large range of scales and thus offers the capability of resolving the subgrid-scale rainfall variability at any selected scale without the need to consider a separate parameterization at each scale. Third, as it was demonstrated in Perica and Foufoula-Georgiou (1996b), this downscaling scheme has the ability to accurately reconstruct the percent of area covered by a storm at all subgrid scales by simply introducing a very low-level rainfall intensity cutoff parameter. All these advantages are missing, for example, from the commonly used simple rainfall subgrid parameterization scheme which consists of prespecifying the fraction of area covered by rain, e.g., 30%, and an exponential distribution with fixed parameters for redistribution of rainfall at the rainy boxes of a desired scale (e.g., see Schaake *et al.* 1996). This scheme typically does not have the ability to dynamically update its parameters as the storm evolves, neither to consider the scale-dependence of these parameters. It should be stressed however, that the advantages of the scheme of Perica and Foufoula-Georgiou (1996b) draw heavily upon two main hypotheses: (a) that standardized rainfall fluctuations exhibit Normality and simple scaling over a significant range of spatial scales, and (b) that there is a strong relationship between the value of CAPE in the prestorm environment (i.e., ahead of the storm development) and the statistical parameterization of standardized rainfall fluctuations. These hypotheses need to be further tested for other storm environments than the ones studied by Perica and Foufoula-Georgiou (1996a, 1996b). Also, while spatial rainfall disaggregation at one instant of time given a large-scale rainfall average might be quite successful with this scheme, it is important to explore how the temporal persistence of the small-scale rainfall variabilities can also be preserved. For that, spatio-temporal scaling models of rain would be very useful and this is an important open problem that needs further investigation.

Although the CAPE *vs*  $H$  and CAPE *vs*  $\sigma_{\xi, 8 \times 8}$  relationships provide a positive first step in linking physics and statistics of rain in a meaningful and practical way, several issues still remain to be further explored to better un-

derstand why they hold in the first place. Unfortunately, data limitations, and especially the lack of frequent soundings at stations within the storm development area, do not permit an empirical investigation of this question. Insights can only be gained from numerical simulation of storms using an atmospheric model which can provide not only values of rainfall intensities at all grid points but also values of CAPE. Such a recent investigation by Zhang and Fofoula-Georgiou (1997) revealed that the spatial variability of CAPE shows a well behaved structure relative to the storm variability and evolution. For example, they found, by numerical simulation of the squall line of June 11, 1985, that the spatial distribution of CAPE was characterized by a large-scale low ( $< 100 \text{ m}^2\text{s}^{-2}$ ) and a few localized high gradient zones ( $> 2000 \text{ m}^2\text{s}^{-2}$ ), which generally coincided with the convergence locations of wind velocity near the ground. As verified against observations, the high convective energy zones correlated very well with the propagation of the squall line.

Such an association of CAPE's spatial pattern change with the squall line development demonstrates that CAPE is a sensitive variable to the meteorological conditions of the storm environment. In fact, that high values of CAPE concentrate at a few locations in front of the squall line development offers promise for the definition of a storm representative value of CAPE based on point values. Specifically, Zhang and Fofoula-Georgiou proposed the use of a representative value of CAPE, denoted by  $\langle \text{CAPE} \rangle$ , as an average of grid point CAPE values exceeding a prespecified threshold which is estimated through comparison with available observations at sparse points of the storm domain. This issue however, needs further careful investigation and in particular the following questions warrant further study: (1) for which storm environments is  $\langle \text{CAPE} \rangle$  a good representative measure of the convective instability in the atmosphere, and for which environments it is not; (2) how does CAPE evolve in the build-up, maturing, and dissipation phases of a storm evolution, and does it offer a representative parameter in all these phases; (3) for what storm types (warm versus cold season midlatitude storms) do the predictive relationships between  $\langle \text{CAPE} \rangle$  and  $H$  and  $\sigma_{\xi, 8 \times 8}$  hold, and for which they do not; and (4) what are the effects of pronounced topography on the subgrid scale rainfall variability, and specifically on scaling of standardized rainfall fluctuations and CAPE spatial distribution?

Another still open problem which is also of mathematical interest is to define the classes of processes ( $X(t)$ ) for which the standardized wavelet fluctuations  $\{X'(t)/\bar{X}(t)\}$  exhibit simple scaling, as they do for spatial rainfall, at least within the tested scales of  $4 \times 4 \text{ km}^2$  to  $64 \times 64 \text{ km}^2$ . (It should be noted that this property has been found to be exhibited by the fluctuations of high resolution temporal rainfall (Venugopal 1996; unpublished manuscript)



only for a short range of scales, approximately 10 secs to 5 mins, which is of the order of decorrelation time for these rainfall series.) Such a development would shed light into the spatial rainfall generating mechanism and would also provide a concise model of rainfall intensities. This problem was presented by us to Daubechies in 1994 (during her visit to the Institute of Mathematics and Applications at the University of Minnesota) and she was intrigued by the presence of such an order in the structure of rainfall fluctuations which certainly is not usual for other processes. For sure this means something about the underlying rainfall process and its generating mechanism and should be further investigated. In trying to relate the structure of the underlying generating mechanism of the process to the scaling structure of their wavelet coefficients, experimentation with exponentiated Brownian motion type models, such as this of Veneziano *et al.* (1996) or the wavelet-based model of Benzi *et al.* (1993) for the construction of multiaffine (anisotropic multifractal) fields might offer a starting point.

## 2.4 Concluding Remarks

As was mentioned in the introduction of this article, this review was not meant to be comprehensive. It focused on selected recent developments and went more in depth on studies related to analysis of high resolution temporal rainfall and studies related to spatial rainfall scaling and relation of scaling and physical parameters of the storm environment. As a result, several recent important advances (several of which can be found in the special *J. Geophysical Research*, Volume 101, issue D21 that resulted from papers presented at the Fifth International Conference on Precipitation) have not been presented herein. It should be noted that research in this area progresses rapidly and promises new exciting results and convergence to a coherent picture especially in integrated space-time rainfall developments.

Apart from the specific open problems in temporal and spatial rainfall research discussed in the previous sections, there are some other fundamental questions which in our opinion need mathematical and empirical investigation. One problem relates to developing a rigorous mathematical framework which can permit to reconcile and integrate model outputs and data at different scales. This problem becomes increasingly important when the results of atmospheric or land-surface models are compared with observables for model validation, and the scales of model outputs is not the same with that of the observables. Such methodologies are in their infancy and they hold much promise for hydrometeorological research in general, and rainfall research in particular. Based on mathematical developments of the group of Willisky at

MIT, Kumar (1997) has recently explored a Kalman filtering approach for information assimilation at different scales. This information can include point measurements, other average observables, or model outputs which are usually considered as averages over the grid boxes of the models. The idea is to replace the time variable in the Kalman filtering approach with a scale variable and develop analogous theories in a multiscale framework.

Another important open problem relates to the understanding of what are the underlying dominant processes and what are the dynamically active structures constituting the rainfall fields. In turbulence, if linear averaging is needed to go from Boltzmann to Navier-Stokes equations, non-linear (conditional) averaging is needed to go from Navier-Stokes to fully developed turbulence equations. An open question in turbulence is how to do this averaging. It is argued (Fargé *et al.* 1996) that one must first identify the dynamically active structures constituting turbulent flows, classify their elementary interactions and define averaging procedures to construct appropriate statistical observables whose evolution is then to be followed and described. If a similar approach is possible to be followed for rainfall, it will not only offer a better understanding of the process, but it will also provide a much needed integration of its space and time dynamics by offering a chance to study temporal rainfall scaling and spatial rainfall scaling features simultaneously. Recent efforts along this direction (e.g., Over and Gupta 1996, Marsan *et al.* 1996, and Venugopal *et al.* 1997) are all based on different approaches and deserve a detailed comparative review in the near future.

## Acknowledgments

The author would like to acknowledge the contribution to this research of several past and current graduate students and collaborators and in particular the contributions of Praveen Kumar, Sanja Perica, Alin Cârsteanu, Venugopal Vuruputur, and Shuxia Zhang. Special thanks go to Alin Cârsteanu and Venugopal Vuruputur for discussions during the writing of this article and help with the preparation of the figures. The author also wishes to thank the organizers of the March, 1996 Mexico workshop on "Stochastic and Statistical Methods in Hydrology". Their hospitality and excellent forum they provided resulted in stimulating discussions and fruitful exchange of ideas. This research was supported over the past several years by NSF (Grants BSC-8957469 and EAR-9117866), NASA (Grant NAG 5-2108) and NOAA (Grant NA46GP0486). We thank the Minnesota Supercomputer Institute for their continuous and generous support of computing resources required for our research. All the rainfall data used in this research are available from the author upon request.

## References

1. Air Weather Service (1979), 'The use of skew T, logP diagram in analysis and forecasting.' Scott AFB, IL 62225.
2. Arnéodo, A., F. Argoul, E. Bacry, J. Elezgaray, E. Freysz, G. Grasseau, J.F. Muzy, and B. Pouligny (1992a), 'Wavelet transform of fractals', in *Wavelets and Some of Their Applications, Proceedings*, edited by Y. Meyer, 286, Springer-Verlag, New York.
3. Arnéodo, A., F. Argoul, J. F. Muzy, and M. Tabard (1992b), 'Uncovering Fibonacci sequences in the fractal morphology of diffusion-limited aggregates', *Phys. Lett. A* **171**, 31-36.
4. Arnéodo, A., F. Argoul, J. F. Muzy, M. Tabard, and E. Barcy (1993), 'Beyond classical multifractal analysis using wavelets: uncovering a multiplicative process hidden in the geometrical complexity of diffusion limited aggregates', *Fractals* **1**(3), 629-649.
5. Arnéodo, A., E. Bacry, and J. F. Muzy (1994), 'Solving the inverse fractal problem from wavelet analysis', *Europhysics Letter*, **25** (7), 479-484.
6. Bacry, E., J. F. Muzy, and A. Arnéodo (1993), 'Singularity spectrum of fractal signals from wavelet analysis: exact results', *J. of Stat. Phys.* **70**, 3, 4, 635-674.
7. Benzi, R., L. Biferale, A. Crisanti, G. Paladin, M. Vergassola, and A. Vulpiani (1993), 'A random process for the construction of multi-affine fields', *Physica* **D65**, 352-358.
8. Cahalan, R. F., M. Nestler, W. Rigway, W. L. Wiscombe, and T. Bell (1990), 'Marine stratocumulus spatial structure', in *Proc. of the 4th Int. Meeting on Statistical Climatology*, ed. J. Sansom, pp 28-32, New Zealand Meteorological Service, Wellington, N.Z.
9. Cârsteanu, A.-A., K.P. Georgakakos, M.B. Sharifi, and J.A. Sperfslage (April 1993), 'Dimensional analysis of local surface-rainfall data with very high temporal resolution' paper presented at the Fourth International Conference on Precipitation: Hydrological and Meteorological Aspects of Rainfall Measurement and Predictability, Iowa City, Iowa.
10. Cârsteanu, A., and E. Foufoula-Georgiou (June 1995), 'Scale invariance in high resolution temporal rainfall: Evidence of anti-symmetry in a cascade model', paper presented at the Fifth International Conference on Precipitation: Space-Time Variability and Dynamics of Rainfall, Elounda, Crete, Greece.
11. Cârsteanu, A., and E. Foufoula-Georgiou (1996), 'Assessing dependence among weights in a multiplicative cascade model of temporal rainfall', *J. Geophys. Res.*, in press.

12. Casdagli, M., D. D. Jardins, S. Eubank, J. D. Farmer, J. Gibson, N. Hunter, and J. Theiler (1995a), 'Nonlinear modeling of chaotic time series: theory and applications', Report LA-UR-91-1637, Los Alamos.
13. Casdagli, M., S. Eubank, J. D. Farmer, J. Gibson (1995b), 'State space representation in the presence of noise', Report LA-UR-91-1637, Los Alamos.
14. Cohen, L. (1995), *Time Frequency Analysis*. Prentice Hall, New Jersey, 299 pages.
15. Cox, D. R., and V. Isham (1997), 'Stochastic spatial-temporal models of rain', this volume.
16. Coifman, R. R., Y. Meyer, and V. Wickerhauser (1992), 'Wavelet analysis and signal processing', in Ruskai *et al.*, *Jones and Bartlett Publishers*, Boston, pp 153-178.
17. Cuning, J. B. (1986), 'The Oklahoma-Kansas preliminary regional experiment for STORM-Central', *Bull. Am. Meteor. Soc.* **67**(12), 1478-1486.
18. Davis, G., Adaptive nonlinear approximations (1994), Ph. D. Thesis, Department of Mathematics, Courant Institute of Mathematical Sciences, New York University.
19. Daubechies, I. (1988), 'Orthonormal bases of compactly supported wavelets', *Commun. on Pure and Applied Mathematics*, **XLI**, 909-996.
20. Daubechies, I. (1992), Ten Lectures on Wavelets, *SIAM*.
21. Davis, G., Adaptive nonlinear approximations (1994), Ph.D. Thesis, Department of Mathematics, Courant Institute of Mathematical Sciences, New York University.
22. Fargé, M., Eric Goirand, Yves Meyer, Frederic Pascal and Wickerhauser, M.V. (1992), 'Improved predictability of two-dimensional turbulent flows using wavelet packet compression', *Fluid Dynamics Research* **10**, 229-250.
23. Fargé, M., Kevlahan, M., Perrier, N., and Goirand, E. (1996), 'Wavelets and Turbulence', *Proceedings of the IEEE, Special Issue on Wavelets*, Vol **84**(4), 639-669.
24. Foufoula-Georgiou, E., and P. Guttorp (1987), 'Compatibility of continuous rainfall occurrence models with discrete rainfall observations', *J. Geophys. Res.*, **92**(D8), 9679-9682.
25. Foufoula-Georgiou, E., and K. Georgakakos (1991), 'Recent advances in space-time precipitation modeling and forecasting', ch. 3 in *Recent Advances in the Modeling of Hydrological Systems*, D. Bowles and E. O'Connell, Eds., Reidel Publ. Co.
26. Foufoula-Georgiou, E., and W. Krajewski (1995), 'Recent advances in rainfall modeling, estimation, and forecasting', *IUGG*, U.S. National Re-

- port 1991-1994 – Contributions in Hydrology.
27. Foufoula-Georgiou, E., and P. Kumar (1994), (eds.), *Wavelets in Geophysics, Wavelet Analysis and its Applications*, Vol. 4, Academic Press, New York.
  28. Gabriel, K. R., and J. Neumann (1962), 'A Markov chain model for daily rainfall occurrences at Tel Aviv', *Quart. J. R. Meteorol. Soc.* **88**, 90-95.
  29. Georgakakos, K.P., A.-A. Cârsteanu, P.L. Sturdevant, and J.A. Kramer (1994), 'Observation and analysis of midwestern rainrates', *J. Appl. Meteorol.*, **33(12)**, 1433-1444.
  30. Grell, G.A, J. Dudhia and D.R. Stauffer (1994), 'A description of the 5th-generation Penn State/NCAR Mesoscale model (MM5)', NCAR technical note, NCAR/TN-398 +STR.
  31. Gupta, V.K., and E. Waymire (1990), 'Multiscaling properties of spatial rainfall and river flow distributions', *J. Geophys. Res.*, **95(D3)**, 1999-2009.
  32. Gupta, V.K., and E. Waymire (1993), 'A statistical analysis of mesoscale rainfall as a random cascade', *J. Appl. Meteorol.*, **32(2)**, 251.
  33. Gupta, V.K., and E. Waymire (June 1995), 'Cascade theory and rainfall statistics: Some results and open problems', paper presented at the Fifth International Conference on Precipitation: Space-Time Variability and Dynamics of Rainfall, Elounda, Crete, Greece.
  34. Harris, D., M. Menadbe, A. Seed and G. Austin (1996), 'Multifractal characterization of rain fields with a strong orographic influence', *J. Geophys. Res.*, **101(D21)**, 26,405-26,414.
  35. Holley R., and E. Waymire (1992), 'Multifractal dimensions and scaling exponents for strongly bounded random cascades', *Ann. Appl. Prob.*, **2**, 819.
  36. Kolmogorov, A.N. (1962), 'A refinement of previous hypothesis concerning the local structure of turbulence in a viscous inhomogeneous fluid at high Reynolds number', *J. Fluid Mech.*, **13**, 82.
  37. Kumar, P., and E. Foufoula-Georgiou (1993a), 'A multicomponent decomposition of spatial rainfall fields: 1. segregation of large and small-scale features., using wavelet transforms', *Water Resour. Res.*, **29(8)**, 2515-2532.
  38. Kumar, P., and E. Foufoula-Georgiou (1993b), 'A multicomponent decomposition of spatial rainfall fields: 2. self-similarity in fluctuations', *Water Resour. Res.*, **29(8)**, 2533-2544.
  39. Kumar, P. (1996), 'Role of coherent structures in the stochastic-dynamic variability of precipitation', *J. Geophys. Res.*, **101(D21)**, 26,393-26,404.
  40. Kumar, P., and E. Foufoula-Georgiou (1997), 'A review of wavelet anal-

- ysis for geophysical applications', *Rev. of Geophys.*, to appear.
41. Kumar, P. (1997), 'A multiple scale state-space model for characterizing subgrid scale variability of near-surface soil moisture', submitted to *IEEE Tras. Geosc. and Remote Sensing*.
  42. Lamperti, J. (1962), Semi-stable stochastic processes, *Trans. Amer. Math. Soc.*, **104**, 62-78.
  43. Lawford, R. G. (1996), 'Temporal variations in the scaling properties of rain echoes during the development of a cold low in Saskatchewan', *J. Appl. Meteor.*, **35**, 796-809.
  44. Mallat, S. (1989a), 'A theory for multiresolution signal decomposition: the wavelet representation', *IEEE Trans. on Pattern Anal. and Mach. Intel.*, **11(7)**, 674-693.
  45. Mallat, S. (Dec. 1989b), 'Multifrequency channel decomposition of images and wavelet models', *IEEE Trans. on Acoustics, Speech and Signal Anal.*, **37(12)**, 2091-2110.
  46. Mallat, S., and Z. Zhang (1993), 'Matching Pursuits with time-frequency dictionaries', *IEEE Trans. Signal Processing*, **41(12)**, 3397-3415.
  47. Marsan, D., D. Schertzer, and S. Lovejoy (1996), 'Causal space-time multifractal processes: Predictability and forecasting of rain fields', *J. Geophys. Res.*, **101(D21)**, 26333-26346.
  48. Menabde, M., A. Seed, D. Harris and G. Austin (1997), 'Self-similar random fields and rainfall simulation', reprint, submitted to *J. Geophys. Res.*.
  49. Menabde, M., D. Harris, A. Seed, G. Austin and D. Stow (1997), 'Multiscaling properties of rainfall and bounded random cascades', reprint, submitted to *Water Resour. Res.*.
  50. Muzy, J. F., E. Bacry, and A. Arnéodo (1994), 'The multifractal formalism revisited with wavelets', *Int. J. of Bifurcation and Chaos*, **4, 2**, 245-302.
  51. Oboukhov, A.M. (1962), 'Some specific features of atmospheric turbulence', *J. Fluid Mech.*, **13**, 77.
  52. Olsson, J., J. Niemczynowicz, and R. Berndtsson (1993), 'Fractal analysis of high-resolution rainfall time series', *J. Geophys. Res.*, **98(D12)**, 23265-23274.
  53. Onof, C and H. Wheater (1993), 'Modeling of British rainfall using a random parameter Bartlett-Lewis rectangular pulse model', *J. of Hydrol.*, **149**, 67-95.
  54. Over, T.M., and V.K. Gupta (1994), 'Statistical analysis of mesoscale rainfall: dependence of a random cascade generator on large-scale forcing', *J. Appl. Meteorol.*, **33(12)**, 1526-1542.

55. Over, T.M., and V.K. Gupta (1996), 'A Space-time theory of mesoscale rainfall using random cascades', *J. Geophys. Res.*, **101(D21)**, 26319-26331.
56. Perica, S., and E. Foufoula-Georgiou(1996a), 'Linkage of scaling and thermodynamic parameters of rainfall: Results from midlatitude mesoscale convective systems', *J. Geophys. Res.*, **101(D3)**, 7431-7448.
57. Perica, S., and E. Foufoula-Georgiou (1996b), 'A model for multiscale disaggregation of spatial rainfall based on coupling meteorological and scaling descriptions', *J. Geophys. Res.*, in press.
58. Robinson, S.K.(1991), 'Coherent motion in turbulent boundary layer', *Annu. Rev. Fluid Mech.*, **23**, 601-639.
59. Rodriguez-Iturbe, I., F. B. De Power, M. B. Sharifi, and K. P. Georgakakos (1989), 'Chaos in Rainfall', *Water Resour. Res.*, **25(7)**, 1667-1675.
60. Ruskai, M. B., G. Beylkin, R. Coifman, I. Daubechies, S. Mallat, Y. Meyer, L. Raphael (1992), eds, *Wavelets and their Applications*, Jones and Bartlett Publishers, Boston.
61. Schaake, J.C., V.I. Koren, Q.-Y. Duan, K. Mitchell and F. Chen (1996), 'Simple water balance model for estimating runoff at different spatial and temporal scales', *J. Geophys. Res.*, **101(D3)**, 7461-7475.
62. Schertzer, D. and S. Lovejoy (1983), 'Elliptical turbulence in the atmosphere', *Proc. of the 4th Symp. on Turbulent Shear Flows*, Nov. 1983, Karlsruhe, Germany.
63. Schertzer, D., and S. Lovejoy (1987), 'Physical modeling and analysis of rain and clouds by anisotropic scaling multiplicative processes', *J. Geophys. Res.*, **92(D8)**, 9693-9714.
64. Shannon, C.E. (1993), *Collected papers*, ed. by N.J.A. Sloane and A.D. Wyner, IEEE Press, New York.
65. Svensson, C., J. Olsson, and R. Berndtsson (1996), 'Multifractal properties of daily rainfall in two different climates', *Water Resour. Res.*, **32(8)**, 2463-2472.
66. Thomas, G. and A. Henderson-Sellers (1991), 'An evaluation of proposed representation of subgrid hydrologic processes in climate models', *J. Climate*, **4**, 898-910.
67. Tessier Y., S. Lovejoy, and D. Schertzer (1993), 'Universal multifractals: Theory and observations for rain and clouds', *J. Appl. Meteor.*, **32(2)**, 223.
68. Veneziano, D., R.L. Bras, and J.D. Niemann (1996), 'Nonlinearity and self-similarity of rainfall in time and a stochastic model', *J. Geophys. Res.*, **101(D21)**, 26,371- 26,392.

69. Venugopal, V. (1995), *Time-Frequency-Scale Analysis of Temporal Rainfall*, M.S. Thesis, Dept. of Civil Engineering, University of Minnesota, Minneapolis.
70. Venugopal V. and E. Foufoula-Georgiou (Dec. 1996), 'Energy decomposition of rainfall in the time-frequency-scale domain', *J. Hydrol.*, 187.
71. Venugopal, V, E. Foufoula-Georgiou, and V. Sapozhnikov (1997), 'Spatio-temporal organization of rainfall fields: A Taylor-like hypothesis for large scales', MSI report, University of Minnesota, June.
72. Warrilow, D.A., A.B. Sangster and A. Slingo (1986), 'Modeling of land-surface processes and their influence on the European climate', *Dynamic Climatology Tech. Note*, 38, 92 pp., Meteorological Office, Bracknell, Berkshire.
73. Waymire, E., V. K. Gupta, and I. Rodriguez-Iturbe (1984), 'A spectral theory of rainfall intensity at the meso- $\beta$  scale', *Water Resour. Res.*, 20, 1453-1465.
74. Wickerhauser, M.V. (1991), *Lectures on wavelet packet algorithms*, Preprint, Dept. of Mathematics, Washington University.
75. Wickerhauser, V, M., Farge, M., Goirand, E., Wesfreid, E., and Cubillo, E. (1994), 'Efficiency comparison of wavelet packet and adapted local cosine bases for compression of a two-dimensional turbulent flow', in *Wavelets : Theory, Algorithms and Applications* edited by Chui, C., Montefusco, L., and Puccio, L., pp 509-531.
76. Wornell, G. M. (1996), *Signal Processing With Fractals: a Wavelet-based Approach*, Prentice Hall, N. J., 177 pgs.
77. Zawadzki, I. I. (1973), 'Statistical properties of precipitation patterns', *J. Appl. Meteor.*, 12, 459-472.
78. Zhang, S. and E. Foufoula-Georgiou (1997), 'Subgrid-scale rainfall variability and its effect on atmospheric and surface variable prediction', *J. Geophys. Res.*, to appear.